

1 **Novel municipal sewage-associated bacterial genomes and their potential in source tracking**

2

3 Blake G. Lindner<sup>1</sup>, Brittany Suttner<sup>1</sup>, Roth E. Conrad<sup>2</sup>, Luis M. Rodriguez-R<sup>1,3</sup>, Janet K. Hatt<sup>1</sup>,

4 Kevin J. Zhu<sup>1</sup>, Joe Brown<sup>1a</sup>, and Konstantinos T. Konstantinidis<sup>1\*</sup>

5

6 <sup>1</sup> School of Civil and Environmental Engineering, Georgia Institute of Technology, Atlanta, GA

7 30332, USA

8 <sup>2</sup> Ocean Science and Engineering, Georgia Institute of Technology, Atlanta, GA 30332, USA

9 <sup>3</sup> Department of Microbiology and Digital Science Center (DiSC), University of Innsbruck, 6020

10 Innsbruck, Tyrol, Austria

11

12 Present address:

13 <sup>a</sup> Department of Environmental Sciences and Engineering, Gillings School of Global Public

14 Health, University of North Carolina at Chapel Hill, North, Carolina, NC 27599, United States

15

16 \* To whom correspondence should be addressed.

17 Konstantinos T. Konstantinidis,

18 311 Ferst Drive, ES&T Building, Room 3321,

19 Georgia Institute of Technology.

20 Atlanta, GA, 30332.

21 Telephone: 404-639-4292

22 Email: [kostas@ce.gatech.edu](mailto:kostas@ce.gatech.edu)

23 **Abstract**

24 Little is known about the genomic diversity of raw municipal wastewater (sewage)  
25 microbial communities, including to what extent sewage-specific populations exist and how they  
26 can be used to improve source attribution and partitioning in sewage-contaminated waters.  
27 Herein, we used the influent of three wastewater treatment plants in Atlanta, Georgia (USA) as  
28 inoculum in multiple controlled laboratory mesocosms to simulate sewage contamination events  
29 and followed these perturbed freshwater microbial communities with metagenomics over a 7-day  
30 observational period. We describe 15 abundant non-redundant bacterial metagenome-assembled  
31 genomes (MAGs) ubiquitous within all sewage inoculum yet absent from the unperturbed  
32 freshwater control at our analytical limit of detection. Tracking the dynamics of populations  
33 represented by these MAGs revealed varied decay kinetics, depending on (inferred) phenotypes,  
34 e.g., anaerobes decayed faster under the well-aerated incubation conditions. Notably, a portion of  
35 these populations show decay patterns similar to common markers, *Enterococcus* and HF183.  
36 Comparisons against MAGs from different sources such as human and animal feces, revealed  
37 low cross-reactivity, indicating how genomic collections could be used to sensitively identify  
38 sewage contamination and partition signal among multiple sources. Overall, our results indicate  
39 the usefulness of metagenomic approaches for assessing sewage contamination in waterbodies  
40 and provides needed methodologies for doing so.

41

## 42 **Introduction**

43 Wastewater collection systems (or simply, collection systems) represent an important  
44 engineering control for the collection of human feces, commercial or industrial wastewaters, and  
45 sometimes stormwater, particularly in certain urban settings. The operation and maintenance of  
46 collection systems pose unique challenges, often due to their size, complexity, and capital costs

47 (1-3). Population growth and distribution changes – especially growing urbanization trends –  
48 highlight the importance of maintaining and expanding efficient collection systems for an  
49 increasing fraction of the global population (4). Severe weather, pipe blockages, aging, and other  
50 issues of system failure can lead to the accidental release of untreated wastewater (sewage) from  
51 collection systems into waterways or floodwaters (1-3,5). As sewage is a significant reservoir of  
52 both chemical and biological pollutants, its release into the environment poses serious  
53 environmental and human health risks, including potential exposure to human pathogens (6-9)  
54 and possible dissemination of antimicrobial resistance genes (ARGs) among microbial  
55 populations (10-12).

56       Microbial source tracking (MST) refers to a collection of forensic tools developed to  
57 identify the presence and source of contamination among multiple probable fecal sources,  
58 including sewage (13). In large part, the technical approaches behind MST methods have been  
59 developed in response to both the difficulty of assaying for the diverse array of relevant human  
60 pathogens as well as the practical need to keep MST methods relatively rapid and inexpensive.  
61 Existing approaches have relied on indicator organisms to imply the presence of fecal pollution  
62 and sometimes as proxies for the presence of human pathogens in fecal contaminated waters.  
63 Specifically, fecal indicator bacteria (FIB) include an aggregation of bacterial populations  
64 considered representatives of microbial communities inhabiting the guts of warm-blooded  
65 animals. Widely used indicator organisms include *Escherichia coli* and *Enterococcus* spp. More  
66 recently, MST genetic markers from distinct bacterial lineages have been used that leverage  
67 known host specificity of distinct populations for source attribution (14). Some markers (e.g.,  
68 HF183 assay targeting a human-associated *Bacteroides* clade) have found effective use in  
69 environmental management strategies as the basis for inferring the amount of sewage present and

70 thereby, a potential array of pathogen concentrations for iterative risk assessment simulations  
71 (15). Yet, the use of FIB and MST gene markers has had challenges: most notably, that the  
72 concentration of most markers are rarely found to co-vary with pathogen concentrations, marker  
73 concentrations fluctuate with sewage age and the capability of FIB to adapt to environmental  
74 conditions can all combine to confound results interpretation (13,16-18).

75         Within recent years, targeted metabarcoding methods have examined sewage and  
76 sewage-contaminated waters via the 16S rRNA gene or the internal transcribed spacer (ITS) for  
77 prokaryotes and fungi, respectively (17,19-21). These studies have revealed a distinct sewage  
78 “microbiome” dominated by taxa that proliferate in collection systems, sometimes far beyond the  
79 abundance of human gut associated populations (22-24). However, these single-gene assays offer  
80 limited resolution to distinguish between environmental or non-environmental strains of the  
81 same species due to the high sequence conservation of the rRNA gene or the ITS region.  
82 Likewise, these methods do not provide information about the gene content associated with  
83 important populations (e.g., emergent pathogens, ARGs) or resolve finer community-wide  
84 compositional shifts (17,25). Therefore, rRNA gene-based approaches are limited with respect to  
85 quantifying health risks associated with the detection of biomarkers or guide the development of  
86 more holistic environmental management criteria (e.g., site specific criteria).

87         Whole genome shotgun sequencing (or metagenomics), which recovers fragments of the  
88 genomes in a sample, have revealed that bacteria and archaea predominantly form sequence-  
89 discrete populations with intra-population genomic sequence relatedness typically ranging from  
90 ~95% to ~100% average nucleotide identity (or ANI) depending on the population considered  
91 (26). Metagenomic approaches offer unique advantages for environmental health monitoring  
92 tasks including: 1) extensive gene content information of abundant populations, 2) precise

93 ecological estimates of relative abundance at the species level and 3) examination of intra-  
94 species diversity (27). Despite its potential for circumventing some of the challenges facing  
95 existing MST and metabarcoding methods, whole genome shotgun sequencing has not been fully  
96 utilized in monitoring municipal sewage pollution. To date, most applications have focused on  
97 understanding the microbiology of biological wastewater treatment, treated effluents and their  
98 receiving waters, or viral populations (12,28,29). In part, this is because it remains unclear how  
99 to best merge the methods and bioinformatics behind metagenomic practices with existing MST  
100 and environmental monitoring paradigms (30). Widespread application of this technology in the  
101 field requires that several outstanding issues be resolved, including the detection limits of  
102 metagenomic analyses, whether whole and/or metagenome-assembled genomes (MAGs) can  
103 serve as source-specific fecal contamination markers and how metagenomic approaches can infer  
104 the relative contribution of various fecal inputs (referred to hereafter as “source partitioning”).

105         Here, we offer a genome-centric view of sewage-related bacterial populations and  
106 explore their relationships with culture and PCR-based markers during a simulated failure of a  
107 collection system (e.g., an overflow event). Specifically, we simulated sewage contamination  
108 events in lake water obtained from a local drinking and recreational use reservoir, Lake Lanier  
109 (GA, USA), within dialysis bag mesocosms that were incubated in darkness for one week.  
110 Shotgun metagenomic sequencing was performed to search for potential sewage-specific  
111 biomarkers, test the effectiveness of genome collections for fecal source attribution and  
112 partitioning, and directly screen for both pathogens and antimicrobial resistance genes. Lastly,  
113 we propose a theoretical analytical limit of detection for metagenomics that could help guide the  
114 future application and interpretation of whole genome shotgun sequencing to these issues.

115

## 116 **Methods**

### 117 Sample collection, mesocosm setup, and sample processing

118 Samples were collected in sterile glass 1 L bottles from the primary influent of three  
119 WWTPs located in the Atlanta Metropolitan region of Georgia (USA) to serve as representatives  
120 of sewage across three different sewersheds. Each sewershed was comprised of collection  
121 systems with separate stormwater and wastewater conveyance (i.e., separate sewers).  
122 Approximately 50 L of surface water from Lake Lanier, Georgia was also collected concurrently.  
123 Hereafter, these sample groups are referred to as sewersheds A, B, and C. All sewage and water  
124 samples were immediately transported to the lab and stored in darkness at 4 °C until mesocosm  
125 setup, which occurred within 24 hours. For mesocosm setup, 40 L tanks were filled with lake  
126 water and a pump installed for aeration. Experimental dialysis bags were prepared with 110 mL  
127 10% (v/v) sewage and lake water mixture and control bags were filled with 110 mL uninoculated  
128 lake water and closed on both ends using polypropylene Spectra/Por clamps (Spectrum  
129 Laboratories). Both experimental (n=12 x 3 sewersheds = 36 bags) and control (n=12 bags)  
130 dialysis bags were then added to the tank. A small headspace of air was left in each bag when  
131 sealing with clamps so that they could float freely in the tank. Dialysis bag pore sizes (6-8 kDa  
132 molecular weight cutoff) permit the transport of small molecules and ions, but bacterial and viral  
133 particles are contained within the bags. Mesocosms were kept in darkness at 22°C throughout the  
134 duration of the experiment. Sampling occurred at 1, 4, and 7 days by retrieving experimental and  
135 control bags from the mesocosm for destructive processing.

136 Mesocosm sampling, DNA extraction and subsequent qPCR analysis occurred as  
137 described previously in Suttner et al (35). Briefly, water samples were passed through 0.45 µm  
138 poly-carbonate (PC) membranes and stored at -80 °C in 2 mL screw cap bead tubes until

139 processed (within 1-3 months). EPA Method 1600 (31) was followed for enumerating volumetric  
140 *Enterococcus* CFUs. DNA was extracted from PC membranes using the Qiagen PowerFecal kit  
141 and following the manufacturer's instructions with only one exception: mechanical cell lysis was  
142 performed by bead beating in two 1-minute intervals using the Biospec Mini-Beadbeater-24 with  
143 icing between intervals. These DNA extractions were used for qPCR with the HF183/BFDRev  
144 assay (32) and a universal 16S rRNA gene qPCR assay (GenBac16S) to quantify 16S rRNA  
145 gene copies across samples (34). Metagenomic sequencing was performed using the Illumina  
146 Nextera XT kit with library average insert size determined on an Agilent 2100 instrument using a  
147 HS DNA kit and library concentrations determined using the Qubit 1 X dsDNA assay. Samples  
148 were then pooled and sequenced on the HiSeq 2500 instrument as described previously (33).

149 All qPCR reactions were run using an Applied Biosystems 7500Fast thermocycler and  
150 the cycling parameters were as follows: 2 min at 50 °C, 10 min at 95 °C, and 40 cycles of 15 sec  
151 at 95 °C and 60 sec at 60 °C. Assay reactions used 2 µL of template DNA in 20 µL qPCR  
152 reactions with the TaqMan Universal PCR Master Mix (Applied Biosystems). The primer and  
153 probe concentrations were 0.25 µM for HF183 assay and 0.3 µM for the GenBac16S assay.  
154 Template DNAs were run undiluted or diluted 5-fold (to remove the effect of PCR inhibitors)  
155 depending on the expected marker concentration and quality of each sample. Further details on  
156 qPCR reaction set up and standard plasmids for absolute quantification are provided in Suttner et  
157 al. (35) and reiterated within the supplement here (**Supplement Table S1**). To test for extraneous  
158 DNA and potential contamination from sample handling, 50 mL of sterile PBS was also filtered  
159 onto PC membranes and processed following the same DNA extraction at every sampling time  
160 point as described above.

161

162 Bioinformatics sequence processing and population genome binning.

163 Short reads were quality trimmed and Nextera adapters removed with Trimmomatic 0.39  
164 (36). Quality trimming was performed to remove poor quality bases along both ends of  
165 sequences and subsequent removal of any sequences below 50 bp in length. *k*-mer based  
166 operation of Nonpareil 3.304 (-T kmer) was used to estimate the fraction of alpha diversity  
167 covered by the sequencing effort of each metagenome (37). Beta diversity across trimmed short  
168 reads was assessed with the default settings of simka 1.5.1 based on Bray-Curtis dissimilarity  
169 values and visualized by principal coordinate analysis (PCoA) (38). Kraken2 was used to assign  
170 taxonomy and estimate simple relative abundance against a custom library, including bacteria,  
171 archaea, viruses, protozoa, human, and fungal reference genomes at the rank of class (39).  
172 Trimmed short reads were assembled individually with IDBA (UD) 1.1.3 and SPAdes (“--meta”)  
173 3.14.0 using *k*-mer sizes between 20 and 127 (40,41). Contigs shorter than 3Kbp were removed  
174 prior to population genome binning, which was performed with MaxBin 2.2.7 and MetaBAT  
175 2.12.1 (42,43). Additionally, in a parallel workflow, trimmed short reads were normalized via the  
176 BBNorm function of the BBtools suite (version 38) to bring read depths between 10-30X  
177 sequencing depth and then subsequently assembled and binned as described above (44). All  
178 resulting metagenome-assembled genomes (MAGs) from both regular and depth-normalized  
179 short read assemblies were dereplicated using MiGA 0.7.24.0 via the derep\_wf function (45).  
180 Groups of MAGs sharing ANI  $\geq$  95% were clustered into species-like populations (hereafter,  
181 “populations”) with representative MAGs for each population selected by highest completeness  
182 and lowest redundancy. Populations with no representative MAG having a MiGA quality score  
183 above 30% and/or redundancies below 5% were excluded from further analysis. Both Traitax  
184 1.1.2 and MicrobeAnnotator were used with default settings to infer potential phenotypes and



185 annotate draft genomes, respectively (46,47). Lastly, MAGs were screened for cross-reactivity  
186 using the FastANI tool to search for other genomes with ANI  $\geq$  95% across a suite of reference  
187 databases (48).

188

### 189 Annotation of sequence data

190 From the PATRIC database, version 3.6.9, 1097 pathogenic bacterial genome accession  
191 IDs were recovered by querying for host name "Human, homo sapiens" and "good" quality. This  
192 included both genomes tagged as "Reference" (n=28) and "Representative" (n=1069) (49). Of  
193 these, 1076 genomes were recoverable from NCBI for use in this study. Abundance estimates of  
194 pathogen genomes were assessed by short read mapping with Magic-BLAST 1.4.0 (-splice F)  
195 (50). Resulting alignments were filtered using minimum cut-off of 70 bp alignment length, 95%  
196 query coverage by alignment and 95% identity to avoid spurious matches. Additionally, for  
197 virulence gene detection, only experimentally verified nucleotide entries in the Virulence Factor  
198 Database (51) were used. Evaluating MAG abundance across the time series was accomplished  
199 similarly using Magic-BLAST 1.4.0, where MAGs were concatenated into a single library to  
200 which reads were competitively mapped. Additionally, DIAMOND 2.0.1 (blastx --ultra-  
201 sensitive) was used to search short reads against the reference gene sequences of pre-compiled  
202 150 bp  $\beta$ -lactamase ROcker models to reliably identify short reads belonging to  $\beta$ -lactamase  
203 encoding genes (52,53). Reads mapping to these reference sequences were selected for best bit-  
204 score alignment and subsequently filtered by ROcker v1.5.2 as described previously (54).

205

### 206 Estimation of limit of detection, and relative or absolute abundance

207 For a reference genome, MAG, or gene to be considered detected in a sample, at least  
208 10% of the target sequence was required to be covered by reads (i.e., breadth of coverage:  
209 hereafter,  $C$ ), as proposed previously for robust detection of targets in metagenomic datasets  
210 (55). Or, as written, the analytical limit of detection (LOD) used here:

211 Eqn 1: *Analytical LOD*:  $C \geq 0.1$

212 The LOD was automatically implemented by calculating sequencing depth and breadth  
213 similarly to Rodriguez-R et al (56) for estimating “Truncated Average Depth” at 80% (hereafter,  
214 the function TAD80). Python scripts used for this approach are available online at:

215 [https://github.com/rotheconrad/00\\_in-situ\\_GeneCoverage](https://github.com/rotheconrad/00_in-situ_GeneCoverage). In short, the TAD80 function  
216 estimates sequencing depth by first sorting genomic positions according to their sequencing  
217 depth and then removing the upper 10% and lower 10% of positions before averaging the  
218 sequencing depth along the remaining 80% of positions. Since truncation of targets with breadth  
219 of coverage near the detection limits (e.g.,  $C \approx 0.1$ ) could introduce artificially lower values, a  
220 quantification threshold was also necessary to avoid systemic underestimation of abundance for  
221 targets near LOD. From Lander and Waterman (57), breadth of coverage ( $C$ ) is related to  
222 sequencing depth ( $\rho$ ) by the following:

223 Eqn 2:  $C = 1 - e^{-\rho}$

224 Thus, for the analytical LOD defined above, the expected sequencing depth ( $\rho$ ) is simply  
225  $-\ln(0.9)$  for targets at detectable limits. We formalize a quantification threshold which measures  
226 whether a target is quantifiable following application of the truncation function (TAD80) with:

227 Eqn 3: *Quantification Threshold*:  $TAD80(\rho) \geq -\ln(0.9)$

228 For simplicity in our metagenomic results, we describe those targets which satisfied the  
229 LOD condition but were below the quantification threshold as targets that were “detected but not  
230 quantifiable” (DNQ).

231 To convert coverage of detected target genomes to absolute abundances (e.g., cells/mL),  
232 the following approach was used. Single copy gene coverage or genome equivalents (GEQ) and  
233 average genome size (AGS) of metagenomes were evaluated using MicrobeCensus 1.1.0 (58).  
234 The 16S rRNA gene-carrying reads were identified and extracted using sortmeRNA 4.2.0 and  
235 the average 16S rRNA gene coverage was estimated as the sum of extracted read lengths divided  
236 by 1540 bp, the average length of the bacterial 16S rRNA gene (59,60). Average 16S rRNA gene  
237 copy number (16S ACN) for each metagenome was determined by the ratio between 16S rRNA  
238 sequencing depth ( $\rho_{16S}$ ) and GEQ:

239 Eqn 4:  $16S\ rRNA\ ACN = \frac{\rho_{16S}}{GEQ}$

240 The copy number of the 16S rRNA gene per mL as quantified by qPCR was divided by  
241 the 16S rRNA ACN to obtain an estimate for the number of cells in each sample, assuming that  
242 one prokaryotic genome was approximately equivalent to one prokaryotic cell:

243 Eqn 5: *Estimated Prokaryotic Cell Density*  $\left(\frac{cells}{mL}\right) = \frac{16S\ rRNA\ \left(\frac{copies}{mL}\right)}{16S\ rRNA\ ACN}$

244 These measures were taken to help control for bias in relative abundance estimation due  
245 to changes in overall microbial load (cells per volume) and 16S rRNA gene ACN variation  
246 throughout the experiment (61,62). Finally, absolute abundances were estimated by multiplying  
247 a population’s genome equivalents by the estimate for the number of cells in a sample. This was  
248 accomplished using the following equation for a given population via the truncated average  
249 sequencing depth [TAD80( $\rho_i$ )], GEQ and total estimated prokaryotic cell density:

250 Eqn 6: *Est. Pop. Cell Density*  $\left(\frac{\text{cells}}{\text{mL}}\right) = \frac{TAD80(\rho)}{GEQ} * \text{Est. Prok. Cell Density} \left(\frac{\text{cells}}{\text{mL}}\right)$

251 Further, an extension of our definitions of LOD was used in tandem with cell density  
252 estimations for theorizing the smallest abundance detectable as a function of GEQ and cell  
253 density via:

254 Eqn 7: *Detectable Pop. Size*  $\left(\frac{\text{cells}}{\text{mL}}\right) \geq \frac{-\ln(0.9)}{GEQ} * \text{Est. Prok. Cell Density} \left(\frac{\text{cells}}{\text{mL}}\right)$

255

## 256 **Results:**

### 257 Culture and qPCR Data

258 Both fecal indicators (*Enterococcus* and HF183) were in the same order of magnitude across the  
259 sewage samples gathered as inoculum for the mesocosms. Sewage from sewersheds A and B  
260 contained counts with averages of 3.7E+04 and 3.1E+04 Enterococci CFUs/100mL and 2.4E+06  
261 and 3.6E+06 HF183 copies/mL, respectively. Within sewershed C, counts were lower having  
262 1.3E+04 Enterococci CFUs/100mL and 1.5E+06 HF183 copies/mL. Similarly, quantification of  
263 the 16S rRNA gene copy number within the inoculum indicated that overall, microbial loads  
264 were lower in sewershed C than sewersheds A and B (**Supplement Figure S1**). Monitoring  
265 Enterococci and HF183 qPCR markers across the mesocosm timeseries revealed that the markers  
266 decreased throughout the experiment in all replicates but were still detectable at day 7 and  
267 remained higher than the established or recommended water quality criteria for recreational use  
268 waters (i.e., 36 CFUs/100mL and 41 HF183 copies/mL). Only the HF183 marker within  
269 sewershed C mesocosm decreased below detection on Day 7 (**Figure 1**). Neither marker was  
270 detected in the (un-inoculated) freshwater sample serving as control at any time point during  
271 mesocosm operation.

272

## 273 Estimated Microbial Load

274 Prokaryotic cell density of the inoculum varied per mesocosm based on quantification of  
275 the 16S rRNA gene (see Methods for details): 1.1E+09, 2.0E+09, and 1.8E+08 cells/mL were  
276 estimated for sewersheds A, B and C, respectively. Following dilution and mixing of the  
277 inoculum into the mesocosms, day 0 estimates for cell densities were 2.0E+07, 1.7E+08, and  
278 2.5E+07 cells/mL. Thereafter, cell density in both sewershed A and sewershed C mesocosm  
279 increased considerably in the first 24 hours to 1.8E+08 and 6.9E+07 estimated cells/mL (a 924%  
280 and 275% increase) while sewershed B decreased to (an estimated) 1.5E+08 cells/mL.  
281 Subsequent time points revealed steady decreases in cell densities approaching the control cell  
282 density at day 7 of 7.9E+05 estimated cells/mL (**Supplement Table S2**).

283

## 284 Metagenomic-based Coverage and Compositional Shifts of the Mesocosms Over Time

285 Between 1.5 Gbp to 3.5 Gbp of data per sample remained following read quality  
286 trimming and adapter removal, which corresponded to a range of 9 to 27 million reads.  
287 Sequencing effort covered between 36 to 67% of expected nucleotide diversity ( $N_d$ ) across all  
288 samples based on the Nonpareil algorithm, which estimates sequence coverage based on the  
289 degree of redundancy among the metagenomic reads available for each dataset (36). This level of  
290 coverage is adequate for comparing the abundance of features (e.g., genomes, genes) across  
291 samples (63).  $N_d$  estimations of the inoculum and control samples were similar, and day 0 values  
292 closely followed that of their respective sources. A decrease in  $N_d$  occurred within the first 24  
293 hours for all three biological replicates; lower diversities were observed in day 1 samples  
294 compared to those for the inoculum, day 0 samples and the control. The sewershed B series

295 increased in diversity for the remaining days while both sewersheds A and C vacillate thereafter  
296 (**Supplement Table S2**).

297 Observations of beta diversity revealed that the earlier timeseries samples (day 0 and day  
298 1) remained quite similar to the inoculum. By day 4, considerable shifts in community  
299 composition were observed driving the sewage contaminated waters closer to the control  
300 (**Supplement Figure S2**). *k*-mer mapping to characterize these community-wide shifts using  
301 Kraken2 at the class level showed the depletion of *Bacteroidia*, *Epsilonproteobacteria*, and  
302 *Clostridia* following inoculation. None of these classes were detectable in the control samples.  
303 An increase of *Gammaproteobacteria* abundance occurred within the first 24 hours across all  
304 replicates after which this class gradually decreased in abundance with time. Additionally,  
305 increases in *Alphaproteobacteria* and *Cytophagia* occurred in later time points (day 4 and day 7),  
306 far beyond the increase observed in the control, suggesting that the later timepoint samples had  
307 not yet fully recovered from perturbation. Class level relative metagenome-based abundances,  
308 qPCR, culture, and cell density estimation results are summarized on **Figure 1**.

309

#### 310 Sewage-associated Population Genome Binning

311 Seven hundred twenty MAGs were recovered from inoculum and timeseries sample  
312 assemblies. The 720 MAGs were dereplicated at the ANI  $\geq$  95% level, resulting in 49 MAGs  
313 representing sequence discrete populations (hereafter, simply “populations”). Competitive read  
314 mapping to the representative MAG of these populations revealed two groupings delineated by  
315 their presence or absence in the inoculum. Of the total 49, 33 populations were detected within  
316 sewage inoculum samples with varying degrees of prevalence across replicates. We selected a  
317 subset of 15 of these 33 populations that were above the quantification threshold in each

318 inoculum sample, which we refer to as “sewage-associated populations”. This selection process  
319 was motivated twofold: First, to focus only on core populations shared between the inoculum  
320 recovered from each sewershed examined herein. Second, as an effort to exclude potentially  
321 noisy, nonspecific, or transient populations from further analysis. The sewage-associated  
322 populations and their representative MAGs are summarized in **Table 1**. Additionally, we  
323 validated our analytical detection and quantification limits using mock data of known  
324 composition to ensure these criteria were suitable for identifying sewage-associated populations  
325 (**Supplement Table S3.A**) (64). We found our approach, as described in Methods (Eqn. 1 and  
326 2), was robust for reducing quantification error and detected targets of known relative abundance  
327 as expected according to sequencing effort and target genome size, except on very limited  
328 occasions when close relatives were present in the sample at frequencies many times greater than  
329 the target genome. (**Supplement Table S3.B,C**).

330 Our collection of ubiquitous sewage-associated populations in sewersheds A, B, and C  
331 inoculum metagenomes were represented by respectively 9.5%, 5.7%, and 13.3% reads and  
332 15.9%, 8.8%, and 19.6% of GEQ. Estimated absolute abundances of these populations varied  
333 across the samples, from a maximum of 4.4E+07 cells/mL (Pop.01, sewershed B) to a minimum  
334 of 2.3E+05 cells/mL (Pop.04, sewershed C). Within the inoculum, the median and mean absolute  
335 abundances of an individual sewage-associated population was 5.3E+06 and 8.4E+06 cells/mL,  
336 respectively. Overall, sewershed C had substantially lower population densities due to the  
337 difference in total microbial load compared to sewersheds A and B, as noted above. Consistently,  
338 the sewage-associated populations presented here capture a larger portion of the metagenomic  
339 samples associated with sewershed C (compared to A or B), further indicating that the sewershed  
340 C samples may have simply had more dilute microbial load at the time of sampling. Overall,

341 these results reveal that this collection of populations consistently represent highly abundant  
342 members of the sewage microbiome across biological replicates and a substantial part of the total  
343 sewage microbial community.

344 Comparison of the corresponding representative MAG sequences against type material in  
345 the MiGA “TypeMat” database (45) revealed several entries with close matches to previously  
346 described taxa at the species level (e.g., >95% ANI) including *Aeromonas caviae* (Pop.15),  
347 *Acidovorax temperans* (Pop.30), *Prevotella copri* (Pop.43), *Bacteroides vulgatus* (Pop.44), and  
348 *Rivicola pingtungensis* (Pop.49). Of the remaining, six populations matched known genus  
349 representatives, potentially representing a novel species of the matching genera. Two populations  
350 matched members of a known family, one to members of a known order, and one to members of  
351 a known class (**Table 1**). The population with the most distant match in the database (Pop.13,  
352 matching class *Bacteroidia*) with 55.1% average amino acid identity (AAI) to *Paludibacter*  
353 *propioncigenes*.

354 Collections of bacterial isolate genomes and/or MAGs from freshwater (56), activated  
355 sludge (65), anaerobic digestors (66), the human gut environments (67), and the broad general-  
356 purpose GEMs catalog (68), were examined to assess specificity between these 15 sewage-  
357 associated populations and other microbiomes. Of these sewage-associated populations, some  
358 (n=11) may belong to species with members also inhabiting non-sewage microbiomes such as  
359 biological wastewater treatment processes or the human gut (**Supplement Table S4**).  
360 Importantly, only a single population, *Moraxella* (Pop.29), was found via these database searches  
361 to match (95.1-95.0% ANI, borderline of universal species cutoff) genomes recovered from  
362 aquatic environments (both marine and freshwater) (47). This finding suggests Population 29



363 could be less effective as an entry in a sewage-specific genomic library utilized for MST  
364 approaches if other *Moraxella* are in high abundance within the pristine environment.

365

### 366 Sewage-associated Population Decay and Putative Phenotyping

367 Overall, all populations experienced rapid decline in estimated cell densities across the  
368 timeseries with most populations below detection limits following day 4. *Acinetobacter sp.*,  
369 *Cloacibacterium sp.*, *Acidovorax temperans*, and *Flavobacterium sp.* (Pop.03, Pop.18, Pop.30  
370 and Pop.33, respectively) were detectable in at least one biological replicate at day 7 but most of  
371 these observations were below quantification. Signal from sewershed A had the greatest  
372 persistence; of the four mesocosms with quantifiable levels of a sewage-associated population by  
373 day 7, three belonged to the series of sewershed A. Notably, *Acidovorax temperans* (Pop.30) was  
374 the only population detected at day 7 in all three sewersheds (**Figure 2**).

375 All populations remaining detectable at day 7 were putatively phenotyped as aerobic or  
376 facultatively anaerobic by Traitair analysis except for *Cloacibacterium sp.* (Pop.18), which could  
377 not be confidently classified. Nonetheless, *Cloacibacterium sp.* belongs to a genus of facultative  
378 anaerobes (*Cloacibacterium*), suggesting that it likely is a facultative population and that the  
379 representative MAG did not contain the necessary genes for confident phenotyping due to  
380 incompleteness. No population – regardless of (predicted) preference for oxygen – showed an  
381 increased estimated cell density outside the first 24 hours of the incubation. All sewage-  
382 associated populations were likely gram negative, rod or oval-shaped bacteria as predicted by  
383 Traitair (**Supplement Figure S4**).

384 MicrobeAnnotator indicated *Acinetobacter sp.* (Pop.03) and *Acidovorax temperans*  
385 (Pop.30) contained modules for aromatic carbon degradation which were rare genomic features

386 among the representative MAGs. *Acinetobacter sp.* (Pop.03) was reported to contain complete  
387 benzoate degradation and catechol ortho-cleavage modules, while *Acidovorax temperans*  
388 (Pop.30) contained complete catechol ortho-cleavage and incomplete catechol meta-cleavage  
389 modules but none for benzoate degradation (**Supplement Figure S5**).

390

### 391 Human Markers vs Sewage-associated Populations

392 Our results suggested that several of the sewage-associated populations are possibly  
393 linked to the human gut microbiome (**Supplement Table S4**). Based on AAI values, Pop.43 and  
394 Pop.44 were assigned to *Bacteroidales* lineages but likely represent a different lineage than that  
395 represented by HF183 based on the 16S rRNA genes carried on these populations' closest  
396 complete genome matches from a cultured representative (See **Table 1**). Modelling the linear  
397 relationship between either HF183 or *Enterococcus* concentrations against the estimated cell  
398 densities of the sewage-associated populations revealed divergent results for both markers.  
399 HF183 had excellent correlations against some populations (i.e., anaerobic Pop.43 and Pop.44,  
400 and aerobic Pop.30 and Pop.28) but highly variable correlations overall ( $R^2$  between 0.35 to  
401 0.97) while *Enterococcus* had worse correlations but with a tighter range ( $R^2$  between 0.5 to 0.8)  
402 (**Figure 3**). As noted above, not all the sewage-associated populations highlighted as potentially  
403 co-habiting the human gut co-varied in abundance as well with HF183 concentrations. For  
404 example, correlations with HF183 concentrations were moderate with the presumed aerobes of  
405 Pop.03 ( $R^2 = 0.69$ ) and Pop.29 ( $R^2 = 0.75$ ) but poor for the facultative Pop.15 ( $R^2 = 0.35$ ).

406

### 407 Genome-based Source Tracking

408           We aimed to demonstrate how read mapping metagenomic data to genome collections  
409 can perform differential source attribution of the fecal contamination within our single input  
410 mesocosm experiments. Our goal was to construct libraries of genomes representing the  
411 microbial pollutants expected to belong to a specific fecal source. To accomplish this, we  
412 downloaded MAGs, isolate genomes, and other reference genomes from several largescale  
413 studies of host microbiomes to create a library for determining source attribution with whole-  
414 genome sequences (67, 69-71) The collected data included genomic entries representing the fecal  
415 microbiomes of humans (n=4644), pigs (n=1667), and chickens (n=5675) and the rumen  
416 microbiome of cows (n=2124). Using MiGA, we dereplicated entries from each collection to  
417 obtain representative genomes with the highest quality for groups of genomic entries with ANI  $\geq$   
418 95% to each other to reduce both the size of the dataset and redundant entries representing highly  
419 similar populations within a collection of host-associated genomes. This approach was the same  
420 as described in our methods for processing and selecting the MAGs described above and shown  
421 on **Table 1**. Using these dereplicated genomes and including the 15 representative MAGs we  
422 produced herein, we searched for and removed any instances of ANI  $\geq$  95% matches across these  
423 collections of host-associated genomes to control for potential cross-reactivity. One exception for  
424 which we did not remove matching genomes was between matching human and sewage genomes  
425 since they represent the same fecal source and would not complicate interpretation of results  
426 (**Supplement Table S4**). Our library construction and curation efforts are summarized in **Figure**  
427 **4**.

428           Next, we aimed to use our host-specific source libraries to perform source attribution and  
429 partitioning as if our mesocosm data represented metagenomes recovered from a waterbody  
430 contaminated by a single unknown source. Thus, we performed competitive read mapping of the

431 metagenomic data to the finalized non-redundant genomic library using Magic-BLAST and  
432 custom scripts for TAD80 calculation as described above for tracking the sewage-associated  
433 populations individually. Resulting TAD80 values were summed within each source category  
434 and normalized to GEQ to allow interpretation of these results as the percentage of contribution  
435 from each fecal source in the form of % GEQ (e.g., percentage of prokaryotic genomes)  
436 belonging to a source (**Figure 5, A**). No source category was detected in the control samples and  
437 signal from our collection of sewage MAGs dominated the timeseries across all sewersheds but  
438 rapidly disappeared after day 4. The combined human signal followed a similar pattern as the  
439 sewage though usually at about 10% less GEQ. The pig, cow, and chicken source categories  
440 were usually not detected or were consistently <0.1% GEQ. Hence, this approach provides the  
441 means to assess contamination at the metagenomic read level, circumventing a substantial  
442 computational burden to assemble, bin and obtain de-replicated MAGs.

443

#### 444 Pathogen and Virulence Genes Assessment

445 To assess the ability of the metagenomic approach to provide insights into the health risk  
446 associated with bacterial pathogens introduced by sewage contamination during mesocosm  
447 operation, we recruited metagenomic short reads to 1076 pathogenic bacterial genomes  
448 recovered from the PATRIC webserver (**Supplement, Table S5**). Results revealed that 63, 38,  
449 and 129 pathogen genomes from sewersheds A, B, and C, respectively within the inoculum had  
450 sequencing depths at or above our established LOD after read mapping (see Methods, Eqn. 1)  
451 (**Supplement, Table S6**). In contrast, immediately following inoculation on day 0 many  
452 reference genomes were no longer detectable, with a total of 61, 25, and 20 pathogenic genomes  
453 detected from sewersheds A, B, and C, respectively. It should be mentioned, for many of these

454 organisms, pathogenicity is a function of genotype (e.g., the *E. coli* pathotypes) and the methods  
455 used herein were developed for species-level detection and not optimized for distinguishing  
456 between closely related genotypes of the same species at low abundances (55).

457 Therefore, due to the low relative abundances of these pathogens that we observed and  
458 the need to assess the actual genetic content present within these populations, we examined the  
459 relative abundance of experimentally verified genes within the Bacterial Virulence Factor  
460 Database (VFDB) as proxies for key bacterial pathogens (**Figure 5, B**). The virulence signal  
461 within inoculum metagenomes primarily comprised those belonging to *Aeromonas*, *Klebsiella*,  
462 and *Shigella* pathogenic genera, consistent with the whole-genome detection results above.  
463 Sewage from both sewershed A and C appeared to have greater virulence factor signals  
464 compared to sewage from sewershed B, which had drastically lower detected levels of  
465 *Aeromonas* VFs and no detection of *Klebsiella*, *Shigella* or *Escherichia* VFs. Within the  
466 sewershed A and C timeseries, average virulence abundance was lower on day 0 than in the  
467 inoculum but quickly reached a maximum in 24 hours before substantially decreasing by day 4  
468 and being below detection by day 7. The increase was primarily due to substantial increase in the  
469 abundance of *Aeromonas hydrophila* VFs. This trend was consistent among genes encoding for  
470 *hlyA* (hemolysin), *aerA* (aerolysin) and *act* (*Aeromonas* enterotoxin), essential cytotoxins for  
471 *Aeromonas* spp. pathogenicity, across the timeseries. Alignment of these three cytotoxin genes to  
472 the MAG representing Pop. 15 revealed that it likely carries a gene encoding for *hlyA* but *aerA*  
473 and *act* were either not binned with the draft genome or truly not carried by this population.  
474 Upon further inquiry, the closest matching entry on NCBI's Genome database was *Aeromonas*  
475 *caviae* NZ\_AP022214 (ANI = 98.0%), which represents a strain isolated from a Japanese  
476 wastewater treatment plant that has not been implicated in disease or designated as an obligate

477 pathogen. Hence, to what extent the MAG identified represents a pathogenic or opportunities  
478 pathogenic population remains somewhat speculative.

479

#### 480 $\beta$ -lactam Resistance Gene Assessment

481 Several classes representing the breadth of  $\beta$ -lactamase-encoding gene diversity were  
482 present in the metagenomes from all samples. The uninoculated lake water (control) sample  
483 showed very low abundance of  $\beta$ -lactamase encoding genes across each class (sum of classes  
484 was 0.078 total  $\beta$ -lactamase encoding genes/genome equivalent) – though a subset of metallo- $\beta$ -  
485 lactamase encoding genes (MBLS3) were noticeably pronounced (0.06 gene copies/genome  
486 equivalent). In the inoculum samples, total observed  $\beta$ -lactamase signal was much greater in  
487 sewersheds A and C (1.07 and 1.14 total gene copies /genome equivalent, respectively)  
488 compared to sewershed B (0.51 total  $\beta$ -lactamase encoding genes/genome equivalent), but the  
489 relative contribution of each class was consistent, with genes encoding for BlaA, BlaC and OXA  
490 dominating. In contrast, by day 4 and to a greater extent by day 7, the frequency of genes  
491 encoding for BlaA, BlaC and OXA decreased consistently while those encoding for MBLs  
492 increased (**Figure 5, C**). Along with a shift in prominence of these  $\beta$ -lactamase gene classes,  
493 both sewersheds A and C showed steep decreases in the relative number of  $\beta$ -lactamase encoding  
494 genes/genome equivalent between day 0 and day 7. Sewershed C showed the same shifts in  
495 prominence between classes, yet total signal remained consistent with 0.55 and 0.54 total  $\beta$ -  
496 lactamase gene copies/genome equivalent on day 0 and 7, respectively.

497

#### 498 **Discussion:**

##### 499 Sewershed Microbial Diversity

500           Collection systems represent a key component of modern sanitation infrastructure.  
501   Despite the importance of sewage as a reservoir for human pathogens and antimicrobial  
502   resistance genes, the sewage microbiome remains relatively understudied at the whole genome  
503   level. Our results indicated that the sewage samples we collected from three separate collection  
504   systems across the Atlanta Metropolitan region were dominated by what have been aptly named  
505   microbial “weeds” in literature and which we have observed as belonging to several sewage-  
506   associated populations which appear quite prolific (21,22). Others have reported many of these  
507   populations are also present at high relative abundances within sewersheds spanning another  
508   urban landscape (72). Our resulting analysis expanded our understanding of these bacterial  
509   populations and their fate during a simulated contamination event by recovering representative  
510   draft genomes (MAGs) for these ubiquitous populations and tracking their abundances over time  
511   with controls in place for microbial load fluctuations. Specifically, we found primary sewage-  
512   associated populations to represent clades within the classes *Gammaproteobacteria* (e.g.,  
513   *Acinetobacter*, *Aeromonas*), *Betaproteobacteria* (e.g., *Acidovorax*, *Rivicola*) and  
514   *Epsilonproteobacteria* (e.g., *Arcobacter*) (**Figure 1,A**).

515           These sewage-associated populations showed different preference for oxygen, appearing  
516   to span strict anaerobic, facultative, and aerobic metabolic phenotypes. Notably, the signal  
517   associated with these populations in the metagenomic datasets decayed non-uniformly during  
518   mesocosm operation, though the most persistent populations were aerotolerant, acetate-utilizing  
519   populations which contained genes related to aromatic degradation and/or nitrogen metabolism.  
520   Depending on additional inquiry, it may be possible to leverage the ratio between abundances of  
521   anaerobic and aerobic (or facultatively anaerobic) sewage-associated populations in future work  
522   for inferring the date of pollution events linked to sewage contamination. For all 15 populations

523 described here, their linear relationship with HF183 and Enterococci had a combined  $R^2$  of 0.6  
524 (**Figure 2**), revealing overall consistent results for different markers under the conditions tested  
525 here. However, these correlations were drawn from the limited number of mesocosm incubations  
526 and *in situ* population dynamics are likely to differ according to varying environmental and  
527 biological factors which were not controlled for herein.

528 Our dataset is of limited size and scope considering that, on a global scale, we examined  
529 sewage from collection systems in essentially equivalent geographies. The assortment of sewage-  
530 associated populations described here, although ubiquitous across the sewersheds we sampled,  
531 likely maintain differing prevalence across time or space. Furthermore, many draft genomes we  
532 produced are not complete, so further work will be needed to establish a more practical view of  
533 both the range of these populations and their genomic content and diversity. Yet, we see  
534 advancing our knowledge of sewage-associated populations as a potential contribution towards  
535 newly developing forensic approaches that help monitor, manage, and repair these essential  
536 infrastructures (73). For example, we observed several highly abundant populations with a range  
537 restricted to only one or two of the three sewersheds. It would be important to gauge whether  
538 populations (or genotypes within a population) exist that are specific to individual sewersheds,  
539 and how the physicochemical characteristics (e.g., municipal vs. industrial waste, flow rates) of  
540 different waste streams might drive the formation of these distinctions. Further inquiry in this  
541 direction may also lead to strategies for resolving source attribution inquiries when multiple  
542 collection systems with differing catchment compositions are all possible sources of  
543 contamination in the same water environment.

544

545 Source Attribution and Partitioning with Host-Specific Genomic Libraries



546           Several of the abundant sewage-associated populations identified above appear closely  
547 related (likely at the species level) to members of human or chicken fecal microbiomes (**Figure**  
548 **4**). Regardless, it appears populations specific to municipal sewage likely exist and represent a  
549 contingent of the sewage microbiome which – if better catalogued – may be useful for  
550 identifying and quantifying sewage pollution in natural ecosystems independent of human-  
551 associated markers. We have demonstrated, through a proof-of-concept workflow, the capacity  
552 for read mapping metagenomic datasets to host-specific genomic libraries for performing both  
553 source attribution and partitioning (**Figure 5, A**). Although source attribution has been well-  
554 developed in existing metagenomic approaches, no metagenomic methods have been developed  
555 which are also capable of simultaneous source partitioning. Here, we have performed source  
556 partitioning for each entry within a host-specific genomic library to a metagenome’s GEQ, which  
557 yields a relatively easy-to-interpret metric describing the percentage of genomes within a  
558 metagenome that belong to a given host or source specific library. We see this as a promising  
559 avenue for metagenomic-based MST methods and believe the approach could eventually be  
560 utilized in the field pending further testing and refinement by mixed input experiments.

#### 561 $\beta$ -lactamase Encoding Genes Surveillance

562           Additionally, we leveraged our metagenomes to survey for  $\beta$ -lactamase genes across the  
563 inoculum and timeseries. The abundance of  $\beta$ -lactamases across the inoculum samples was  
564 substantially higher (7-15 times) compared to the control (**Figure 5**). This result was consistent  
565 with both our expectations and the literature regarding heightened ARG abundance within  
566 collection systems (74). Specifically, others have reported substantial abundances of  $\beta$ -  
567 lactamase OXA genes on both *Campylobacteraceae* and *Aeromonadaceae* clades in sewage (75).  
568 Indeed, the abundance of reads belonging to  $\beta$ -lactamase encoding genes, especially of the OXA-

569 encoding class, were the most abundant in the inoculum and early time points where these  
570 sewage-associated clades (e.g., Pop.01, Pop.19) persisted in the lake water. Overall, these results  
571 indicated that sewage contamination imparted a substantial and lasting increase to the abundance  
572 of genes encoding  $\beta$ -lactamases even after 7 days following the contamination event. More work  
573 is needed to elucidate the genomic context of this increased  $\beta$ -lactamase encoding gene  
574 abundance (e.g., whether they belong to or have been transferred to organisms capable of driving  
575 clinically relevant cases of antimicrobial resistance). Nonetheless, our results allow for a  
576 quantitative view of the abundance of these genes relative to the natural environment where the  
577 freshwater used in the mesocosm incubations originated, which is relevant for assessing the  
578 associated public health risk.

579

#### 580 Pathogen and Virulence Gene Surveillance

581       Importantly, although Sewershed A and B showed what appears to be similar  
582 concentrations of human input according to HF183 concentrations within the inoculum  
583 (**Supplement Figure S1**), the pathogen detection results revealed via the sequence data were  
584 quite varied (**Figure 4B, Supplement Table S6**). Results from both read mapping to bacterial  
585 pathogen genomes and the experimentally verified VFDB collection were consistent in  
586 suggesting that bacterial virulence was more elevated in the Sewershed A inoculum compared to  
587 Sewershed B. This contrast between sewersheds with equal human marker concentrations yet  
588 apparently unequal bacterial pathogen load illustrates how shotgun sequence data can facilitate  
589 perspectives on the actual co-variance of marker and pathogen. Yet these insights clearly depend  
590 on sufficient sequencing effort and/or relatively high pathogen concentrations to avoid the  
591 possibility of false negative results.

592 In particular, the estimated smallest detectable population size associated with our  
593 analysis and sequencing effort ranged between approximately 2E+05 to 1E+02 cells/mL based  
594 on qPCR-based cell count normalization and the sequencing effort applied (Methods,  
595 **Supplement Table S2**). Approaches for estimating analytical LOD within metagenomic based  
596 analysis remain rare within the literature especially as it relates to work done in the environment  
597 as opposed to clinical settings (76,77). Yet, the concept of detection and quantification limits in  
598 metagenomics is a major challenge to its thorough incorporation into environmental monitoring  
599 approaches because 1) it is necessary to track biomarkers or pathogens down to quite low  
600 relative abundance in the field (i.e., <1E-09 target basepairs/total basepairs), and 2) leveraging  
601 extraordinary sequencing effort is currently expensive and not practical when limitations of  
602 expertise and computational resources exist. Our approach provides the means to establish  
603 theoretical analytical LOD for metagenomic analyses based on sequencing effort which is useful  
604 for determining and interpreting the meaning of “non-detects”.

605 Using AGS and total cell density estimates within the inoculum, we estimate  
606 approximately 3.5Tb of sequencing effort is necessary for detecting a population with  
607 concentration of 1E+02 cells/mL within the high microbial loading conditions observed in the  
608 inoculum. In contrast, following the decline in cell density and increase in AGS across the  
609 timeseries, the estimated sequencing effort required to detect a population of 1E+02 cells/mL  
610 drops to 10Gb in day 7 conditions. Therefore, our approach and results reported here for  
611 sequencing effort estimation may be helpful for informing the planning and execution of future  
612 environmental monitoring work utilizing metagenomic approaches (**Supplement Table S7**).  
613 Though, crucial to note is the fact that our approaches for analytical LOD, and sequencing effort  
614 estimation assumes unbiased sequencing and does not consider sampling or processing

615 recoveries – where the latter limitation is obviously broadly applicable to all molecular methods.  
616 Total detection limits, in the context of analytical limits as well as both sequencing bias and  
617 sampling/processing recoveries, will be important caveats to consider for future metagenomic  
618 workflows aiming to surveil pathogens in sewage collection systems or their releases into the  
619 environment (78).

620 While we do not envision that PCR and culturing will be replaced by metagenomics for  
621 routine monitoring because the former techniques are cheaper, easier to analyze, and have a  
622 greater dynamic range of detection – our results do show how metagenomics can provide unique  
623 insights into sewage pollution events such as differential pathogen content of different sewage or  
624 possibly distinguishing between different sewersheds potentially contributing to contamination.  
625 Further, we have shown how metagenomics could track a broad range of population sizes –  
626 about six orders of magnitude (from about  $1E+01$  to  $1E+07$  cells/mL) – which is adequate for  
627 certain applications and/or high-volume pollution events.

628

## 629 Conclusions

630 Our efforts have shown how metagenomic datasets can provide insights on multiple  
631 questions critical to environmental monitoring and water quality: pathogen detection, source  
632 attribution and partitioning, and ARG persistence in the environment. In our view, confident and  
633 direct detection of pathogens within metagenomic datasets will remain primarily a logistical  
634 challenge due to the large amount of sequencing effort required to reliably detect bacterial  
635 pathogens at concentrations that are very low yet still quite relevant to protecting public health.  
636 Thus, when performed alone, metagenomic approaches are unlikely to be the most prudent  
637 technology for routine monitoring and directly informing health risks associated with sewage

638 contamination, especially when pathogen or virulence genes are at these relatively low  
639 abundances (e.g., below 1E+02 features/mL). This issue is also compounded by the large  
640 contribution of non-bacterial pathogens (e.g., viruses and protozoa) to illness risk in  
641 contaminated waters. In contrast, metagenomic approaches are increasingly poised to resolve  
642 questions related to source attribution and partitioning by improving our understanding (and the  
643 size of our databases) of the genomes maintained by source-specific microbial populations.

644

645 **Acknowledgments:**

646 The authors would like to thank the Cobb County Water System, Gwinnett County Department  
647 of Water Resources, and the City of Atlanta Department of Watershed Management for  
648 assistance with this work. This research was supported in part through research  
649 cyberinfrastructure resources and services provided by the Partnership for an Advanced  
650 Computing Environment (PACE) at the Georgia Institute of Technology, Atlanta, Georgia, USA.  
651 This work was supported by the US National Science Foundation, award numbers 1511825 (to  
652 J.B and K.T.K) and 1831582 (K.T.K.) and the US National Science Foundation Graduate  
653 Research Fellowship under grant number DGE-1650044 (to B.S.). The funding agencies had no  
654 role in the study design, data collection and analysis, decision to publish, or preparation of the  
655 manuscript.

656

657 **Conflict of interest:** The authors declare no conflict of interest.

## References

- (1) Salman, B.; Salem, O. Modeling Failure of Wastewater Collection Lines Using Various Section-Level Regression Models. *Journal of Infrastructure Systems* **2012**, *18* (2), 146–154.  
[https://doi.org/10.1061/\(ASCE\)IS.1943-555X.0000075](https://doi.org/10.1061/(ASCE)IS.1943-555X.0000075).
- (2) Berendes, D. M.; Yang, P. J.; Lai, A.; Hu, D.; Brown, J. Estimation of Global Recoverable Human and Animal Faecal Biomass. *Nature Sustainability* **2018**, *1* (11), 679–685.  
<https://doi.org/10.1038/s41893-018-0167-0>.
- (3) McLellan, S. L.; Sauer, E. P.; Corsi, S. R.; Bootsma, M. J.; Boehm, A. B.; Spencer, S. K.; Borchardt, M. A. Sewage Loading and Microbial Risk in Urban Waters of the Great Lakes. *Elementa: Science of the Anthropocene* **2018**, *6* (46). <https://doi.org/10.1525/elementa.301>.
- (4) ten Veldhuis, J. A. E.; Clemens, F. H. L. R.; Sterk, G.; Berends, B. R. Microbial Risks Associated with Exposure to Pathogens in Contaminated Urban Flood Water. *Water Research* **2010**, *44* (9), 2910–2918. <https://doi.org/10.1016/j.watres.2010.02.009>.
- (5) Olds, H. T.; Corsi, S. R.; Dila, D. K.; Halmo, K. M.; Bootsma, M. J.; McLellan, S. L. High Levels of Sewage Contamination Released from Urban Areas after Storm Events: A Quantitative Survey with Sewage Specific Bacterial Indicators. *PLOS Medicine* **2018**, *15* (7), e1002614.  
<https://doi.org/10.1371/journal.pmed.1002614>.
- (6) Ashbolt, N. J.; Schoen, M. E.; Soller, J. A.; Roser, D. J. Predicting Pathogen Risks to Aid Beach Management: The Real Value of Quantitative Microbial Risk Assessment (QMRA). *Water Research* **2010**, *44* (16), 4692–4703. <https://doi.org/10.1016/j.watres.2010.06.048>.
- (7) Fouz, N.; Pangesti, K. N. A.; Yasir, M.; Al-Malki, A. L.; Azhar, E. I.; Hill-Cawthorne, G. A.; Abd El Ghany, M. The Contribution of Wastewater to the Transmission of Antimicrobial Resistance in

the Environment: Implications of Mass Gathering Settings. *Trop Med Infect Dis* **2020**, 5 (1).

<https://doi.org/10.3390/tropicalmed5010033>.

- (8) Medina, W. R. M.; Eramo, A.; Tu, M.; Fahrenfeld, N. L. Sewer Biofilm Microbiome and Antibiotic Resistance Genes as Function of Pipe Material, Source of Microbes, and Disinfection: Field and Laboratory Studies. *Environ. Sci.: Water Res. Technol.* **2020**, 6 (8), 2122–2137.

<https://doi.org/10.1039/D0EW00265H>.

- (9) Eisenberg, J. N. S.; Bartram, J.; Wade, T. J. The Water Quality in Rio Highlights the Global Public Health Concern Over Untreated Sewage. *Environ Health Perspect* **2016**, 124 (10), A180–A181.

<https://doi.org/10.1289/EHP662>.

- (10) Su, X.; Liu, T.; Beheshti, M.; Prigiobbe, V. Relationship between Infiltration, Sewer Rehabilitation, and Groundwater Flooding in Coastal Urban Areas. *Environ Sci Pollut Res* **2020**, 27 (13),

14288–14298. <https://doi.org/10.1007/s11356-019-06513-z>.

- (11) Kessler, R. Stormwater Strategies: Cities Prepare Aging Infrastructure for Climate Change. *Environ Health Perspect* **2011**, 119 (12), a514–a519. <https://doi.org/10.1289/ehp.119-a514>.

- (12) Lira, F.; Vaz-Moreira, I.; Tamames, J.; Manaiá, C. M.; Martínez, J. L. Metagenomic Analysis of an Urban Resistome before and after Wastewater Treatment. *Scientific Reports* **2020**, 10 (1), 8174.

<https://doi.org/10.1038/s41598-020-65031-y>.

- (13) Harwood, V. J.; Staley, C.; Badgley, B. D.; Borges, K.; Korajkic, A. Microbial Source Tracking Markers for Detection of Fecal Contamination in Environmental Waters: Relationships between Pathogens and Human Health Outcomes. *FEMS Microbiol Rev* **2014**, 38 (1), 1–40.

<https://doi.org/10.1111/1574-6976.12031>.

- (14) Bernhard, A. E.; Field, K. G. A PCR Assay To Discriminate Human and Ruminant Feces on the Basis of Host Differences in Bacteroides-Prevotella Genes Encoding 16S RRNA. *Appl. Environ. Microbiol.* **2000**, *66* (10), 4571–4574. <https://doi.org/10.1128/AEM.66.10.4571-4574.2000>.
- (15) Boehm, A. B.; Soller, J. A.; Shanks, O. C. Human-Associated Fecal Quantitative Polymerase Chain Reaction Measurements and Simulated Risk of Gastrointestinal Illness in Recreational Waters Contaminated with Raw Sewage. *Environ. Sci. Technol. Lett.* **2015**, *2* (10), 270–275. <https://doi.org/10.1021/acs.estlett.5b00219>.
- (16) Korajkic, A.; McMinn, B. R.; Harwood, V. J. Relationships between Microbial Indicators and Pathogens in Recreational Water Settings. *Int J Environ Res Public Health* **2018**, *15* (12). <https://doi.org/10.3390/ijerph15122842>.
- (17) Ahmed, W.; Hughes, B.; Harwood, V. J. Current Status of Marker Genes of Bacteroides and Related Taxa for Identifying Sewage Pollution in Environmental Waters. *Water* **2016**, *8* (6), 231. <https://doi.org/10.3390/w8060231>.
- (18) Fecal Indicator Bacteria from Environmental Sources; Strategies for Identification to Improve Water Quality Monitoring. *Water Research* 2020, *185*, 116204. <https://doi.org/10.1016/j.watres.2020.116204>.
- (19) Unno, T.; Staley, C.; Brown, C. M.; Han, D.; Sadowsky, M. J.; Hur, H.-G. Fecal Pollution: New Trends and Challenges in Microbial Source Tracking Using next-Generation Sequencing: Progress and Challenges in MST. *Environ Microbiol* **2018**, *20* (9), 3132–3140. <https://doi.org/10.1111/1462-2920.14281>.
- (20) McLellan, S. L.; Eren, A. M. Discovering New Indicators of Fecal Pollution. *Trends in Microbiology* **2014**, *22* (12), 697–706. <https://doi.org/10.1016/j.tim.2014.08.002>.



- (21) Assress, H. A.; Selvarajan, R.; Nyoni, H.; Ntushelo, K.; Mamba, B. B.; Msagati, T. A. M. Diversity, Co-Occurrence and Implications of Fungal Communities in Wastewater Treatment Plants. *Scientific Reports* **2019**, *9* (1), 14056. <https://doi.org/10.1038/s41598-019-50624-z>.
- (22) Newton, R. J.; McLellan, S. L.; Dila, D. K.; Vineis, J. H.; Morrison, H. G.; Eren, A. M.; Sogin, M. L. Sewage Reflects the Microbiomes of Human Populations. *mBio* **2015**, *6* (2). <https://doi.org/10.1128/mBio.02574-14>.
- (23) McLellan, S.L.; Roguet, A. The Unexpected Habitat in Sewer Pipes for the Propagation of Microbial Communities and Their Imprint on Urban Waters. *Current Opinion in Biotechnology* **2019**, *57*, 34–41. <https://doi.org/10.1016/j.copbio.2018.12.010>.
- (24) McLellan, S. L.; Huse, S. M.; Mueller-Spitz, S. R.; Andreishcheva, E. N.; Sogin, M. L. Diversity and Population Structure of Sewage Derived Microorganisms in Wastewater Treatment Plant Influent. *Environ Microbiol* **2010**, *12* (2), 378–392. <https://doi.org/10.1111/j.1462-2920.2009.02075.x>.
- (25) Poretsky, R.; Rodriguez-R, L. M.; Luo, C.; Tsementzi, D.; Konstantinidis, K. T. Strengths and Limitations of 16S rRNA Gene Amplicon Sequencing in Revealing Temporal Microbial Community Dynamics. *PLOS ONE* **2014**, *9* (4), e93827. <https://doi.org/10.1371/journal.pone.0093827>.
- (26) Caro-Quintero, A.; Konstantinidis, K. T. Bacterial Species May Exist, Metagenomics Reveal. *Environmental Microbiology* 2012, *14* (2), 347–355. <https://doi.org/https://doi.org/10.1111/j.1462-2920.2011.02668.x>.
- (27) Segata, N. On the Road to Strain-Resolved Comparative Metagenomics. *mSystems* **2018**, *3* (2), e00190-17, /msystems/3/2/msys.00190-17.atom. <https://doi.org/10.1128/mSystems.00190-17>.

- (28) Cai, L.; Zhang, T. Detecting Human Bacterial Pathogens in Wastewater Treatment Plants by a High-Throughput Shotgun Sequencing Technique. *Environ. Sci. Technol.* **2013**, *47* (10), 5433–5441. <https://doi.org/10.1021/es400275r>.
- (29) Bibby, K.; Peccia, J. Identification of Viral Pathogen Diversity in Sewage Sludge by Metagenome Analysis. *Environ. Sci. Technol.* **2013**, *47* (4), 1945–1951. <https://doi.org/10.1021/es305181x>.
- (30) Hong, P.-Y.; Mantilla-Calderon, D.; Wang, C. Metagenomics as a Tool To Monitor Reclaimed-Water Quality. *Appl Environ Microbiol* **2020**, *86* (16), e00724-20, /aem/86/16/AEM.00724-20.atom. <https://doi.org/10.1128/AEM.00724-20>.
- (31) USEPA. Method 1600: Enterococci in Water by Membrane Filtration Using Membrane-*Enterococcus* Indoxyl- $\beta$ -D-Glucoside Agar (MEI). United States Environmental Protection Agency 2009.
- (32) Wade, T. J.; Sams, E.; Brenner, K. P.; Haugland, R.; Chern, E.; Beach, M.; Wymer, L.; Rankin, C. C.; Love, D.; Li, Q.; Noble, R.; Dufour, A. P. Rapidly Measured Indicators of Recreational Water Quality and Swimming-Associated Illness at Marine Beaches: A Prospective Cohort Study. *Environmental Health* **2010**, *9* (1), 66. <https://doi.org/10.1186/1476-069X-9-66>.
- (33) Johnston, E. R.; Kim, M.; Hatt, J. K.; Phillips, J. R.; Yao, Q.; Song, Y.; Hazen, T. C.; Mayes, M. A.; Konstantinidis, K. T. Phosphate Addition Increases Tropical Forest Soil Respiration Primarily by Deconstraining Microbial Population Growth. *Soil Biology and Biochemistry* **2019**, *130*, 43–54. <https://doi.org/10.1016/j.soilbio.2018.11.026>.
- (34) Ritalahti, K. M.; Amos, B. K.; Sung, Y.; Wu, Q.; Koenigsberg, S. S.; Löffler, F. E. Quantitative PCR Targeting 16S rRNA and Reductive Dehalogenase Genes Simultaneously Monitors Multiple Dehalococcoides Strains. *AEM* **2006**, *72* (4), 2765–2774. <https://doi.org/10.1128/AEM.72.4.2765-2774.2006>.

- (35) Suttner, B.; Lindner, B. G.; Kim, M.; Conrad, R. E.; Rodriguez, L. M.; Orellana, L. H.; Johnston, E. R.; Hatt, J. K.; Zhu, K. J.; Brown, J.; Konstantinidis, K. T. Metagenome-Based Comparisons of Decay Rates and Host-Specificity of Fecal Microbial Communities for Improved Microbial Source Tracking. *bioRxiv* 2021, 2021.06.17.448865. <https://doi.org/10.1101/2021.06.17.448865>.
- (36) Bolger, A. M.; Lohse, M.; Usadel, B. Trimmomatic: A Flexible Trimmer for Illumina Sequence Data. *Bioinformatics* **2014**, *30* (15), 2114–2120. <https://doi.org/10.1093/bioinformatics/btu170>.
- (37) Rodriguez-R, L. M.; Gunturu, S.; Tiedje, J. M.; Cole, J. R.; Konstantinidis, K. T. Nonpareil 3: Fast Estimation of Metagenomic Coverage and Sequence Diversity. *mSystems* **2018**, *3* (3), e00039-18, /msystems/3/3/msys.00039-18.atom. <https://doi.org/10.1128/mSystems.00039-18>.
- (38) Benoit, G.; Peterlongo, P.; Mariadassou, M.; Drezen, E.; Schbath, S.; Lavenier, D.; Lemaitre, C. Multiple Comparative Metagenomics Using Multiset  $k$ -Mer Counting. *PeerJ Computer Science* **2016**, *2*, e94. <https://doi.org/10.7717/peerj-cs.94>.
- (39) Wood, D. E.; Lu, J.; Langmead, B. Improved Metagenomic Analysis with Kraken 2. *Genome Biol* **2019**, *20* (1), 257. <https://doi.org/10.1186/s13059-019-1891-0>.
- (40) Peng, Y.; Leung, H. C. M.; Yiu, S. M.; Chin, F. Y. L. IDBA-UD: A de Novo Assembler for Single-Cell and Metagenomic Sequencing Data with Highly Uneven Depth. *Bioinformatics* **2012**, *28* (11), 1420–1428. <https://doi.org/10.1093/bioinformatics/bts174>.
- (41) Prjibelski, A.; Antipov, D.; Meleshko, D.; Lapidus, A.; Korobeynikov, A. Using SPAdes De Novo Assembler. *Current Protocols in Bioinformatics* **2020**, *70* (1). <https://doi.org/10.1002/cpbi.102>.
- (42) Wu, Y.-W.; Simmons, B. A.; Singer, S. W. MaxBin 2.0: An Automated Binning Algorithm to Recover Genomes from Multiple Metagenomic Datasets. *Bioinformatics* **2016**, *32* (4), 605–607. <https://doi.org/10.1093/bioinformatics/btv638>.

- (43) Kang, D. D.; Li, F.; Kirton, E.; Thomas, A.; Egan, R.; An, H.; Wang, Z. MetaBAT 2: An Adaptive Binning Algorithm for Robust and Efficient Genome Reconstruction from Metagenome Assemblies. *PeerJ* **2019**, *7*. <https://doi.org/10.7717/peerj.7359>.
- (44) Bushnell, B. *BBMap: A Fast, Accurate, Splice-Aware Aligner*; LBNL-7065E; Lawrence Berkeley National Lab. (LBNL), Berkeley, CA (United States), 2014.
- (45) Rodriguez-R, L. M.; Gunturu, S.; Harvey, W. T.; Rosselló-Mora, R.; Tiedje, J. M.; Cole, J. R.; Konstantinidis, K. T. The Microbial Genomes Atlas (MiGA) Webserver: Taxonomic and Gene Diversity Analysis of Archaea and Bacteria at the Whole Genome Level. *Nucleic Acids Res* **2018**, *46* (Web Server issue), W282–W288. <https://doi.org/10.1093/nar/gky467>.
- (46) Weimann, A.; Mooren, K.; Frank, J.; Pope, P. B.; Bremges, A.; McHardy, A. C. From Genomes to Phenotypes: TraitAr, the Microbial Trait Analyzer. *mSystems* **2016**, *1* (6). <https://doi.org/10.1128/mSystems.00101-16>.
- (47) Ruiz-Perez, C. A.; Conrad, R. E.; Konstantinidis, K. T. MicrobeAnnotator: A User-Friendly, Comprehensive Functional Annotation Pipeline for Microbial Genomes. *BMC Bioinformatics* **2021**, *22* (1), 11. <https://doi.org/10.1186/s12859-020-03940-5>.
- (48) Jain, C.; Rodriguez-R, L. M.; Phillippy, A. M.; Konstantinidis, K. T.; Aluru, S. High Throughput ANI Analysis of 90K Prokaryotic Genomes Reveals Clear Species Boundaries. *Nature Communications* **2018**, *9* (1), 5114. <https://doi.org/10.1038/s41467-018-07641-9>.
- (49) Davis, J. J.; Wattam, A. R.; Aziz, R. K.; Brettin, T.; Butler, R.; Butler, R. M.; Chlenski, P.; Conrad, N.; Dickerman, A.; Dietrich, E. M.; Gabbard, J. L.; Gerdes, S.; Guard, A.; Kenyon, R. W.; Machi, D.; Mao, C.; Murphy-Olson, D.; Nguyen, M.; Nordberg, E. K.; Olsen, G. J.; Olson, R. D.; Overbeek, J. C.; Overbeek, R.; Parrello, B.; Pusch, G. D.; Shukla, M.; Thomas, C.; VanOeffelen, M.; Vonstein, V.; Warren, A. S.; Xia, F.; Xie, D.; Yoo, H.; Stevens, R. The

- PATRIC Bioinformatics Resource Center: Expanding Data and Analysis Capabilities. *Nucleic Acids Research* **2020**, *48* (D1), D606–D612. <https://doi.org/10.1093/nar/gkz943>.
- (50) Boratyn, G. M.; Thierry-Mieg, J.; Thierry-Mieg, D.; Busby, B.; Madden, T. L. Magic-BLAST, an Accurate RNA-Seq Aligner for Long and Short Reads. *BMC Bioinformatics* **2019**, *20* (1), 405. <https://doi.org/10.1186/s12859-019-2996-x>.
- (51) Liu, B.; Zheng, D.; Jin, Q.; Chen, L.; Yang, J. VFDB 2019: A Comparative Pathogenomic Platform with an Interactive Web Interface. *Nucleic Acids Res* 2019, *47* (D1), D687–D692. <https://doi.org/10.1093/nar/gky1080>.
- (52) Buchfink, B.; Xie, C.; Huson, D. H. Fast and Sensitive Protein Alignment Using DIAMOND. *Nat Methods* **2015**, *12* (1), 59–60. <https://doi.org/10.1038/nmeth.3176>.
- (53) Zhang, S.-Y.; Suttner, B.; Rodriguez-R, L.; Orellana, L.; Rowell, J.; Webb, H.; Williams-Newkirk, A.; Huang, A.; Konstantinidis, K. *Rocker Models for Reliable Detection and Typing of Short Read Sequences Carrying  $\beta$ -Lactamases*; preprint; In Review, 2020. <https://doi.org/10.21203/rs.3.rs-113339/v1>.
- (54) Orellana, L. H.; Rodriguez-R, L. M.; Konstantinidis, K. T. ROcker: Accurate Detection and Quantification of Target Genes in Short-Read Metagenomic Data Sets by Modeling Sliding-Window Bitscores. *Nucleic Acids Research* **2017**, *45* (3), e14–e14. <https://doi.org/10.1093/nar/gkw900>.
- (55) Castro, J. C.; Rodriguez-R, L. M.; Harvey, W. T.; Weigand, M. R.; Hatt, J. K.; Carter, M. Q.; Konstantinidis, K. T. ImGLAD: Accurate Detection and Quantification of Target Organisms in Metagenomes. *PeerJ* **2018**, *6*. <https://doi.org/10.7717/peerj.5882>.
- (56) Rodriguez-R, L. M.; Tsementzi, D.; Luo, C.; Konstantinidis, K. T. Iterative Subtractive Binning of Freshwater Chronoseries Metagenomes Identifies over 400 Novel Species and Their Ecologic

- Preferences. *Environ Microbiol* **2020**, 22 (8), 3394–3412. <https://doi.org/10.1111/1462-2920.15112>.
- (57) Lander, E. S.; Waterman, M. S. Genomic Mapping by Fingerprinting Random Clones: A Mathematical Analysis. *Genomics* **1988**, 2 (3), 231–239. [https://doi.org/10.1016/0888-7543\(88\)90007-9](https://doi.org/10.1016/0888-7543(88)90007-9).
- (58) Nayfach, S.; Pollard, K. S. Average Genome Size Estimation Improves Comparative Metagenomics and Sheds Light on the Functional Ecology of the Human Microbiome. *Genome Biology* **2015**, 16 (1), 51. <https://doi.org/10.1186/s13059-015-0611-7>.
- (59) Kopylova, E.; Noé, L.; Touzet, H. SortMeRNA: Fast and Accurate Filtering of Ribosomal RNAs in Metatranscriptomic Data. *Bioinformatics* **2012**, 28 (24), 3211–3217. <https://doi.org/10.1093/bioinformatics/bts611>.
- (60) Wang, Q.; Garrity, G. M.; Tiedje, J. M.; Cole, J. R. Naïve Bayesian Classifier for Rapid Assignment of rRNA Sequences into the New Bacterial Taxonomy. *Appl Environ Microbiol* **2007**, 73 (16), 5261–5267. <https://doi.org/10.1128/AEM.00062-07>.
- (61) Lin, H.; Peddada, S. D. Analysis of Compositions of Microbiomes with Bias Correction. *Nature Communications* **2020**, 11 (1), 3514. <https://doi.org/10.1038/s41467-020-17041-7>.
- (62) Morton, J. T.; Marotz, C.; Washburne, A.; Silverman, J.; Zaramela, L. S.; Edlund, A.; Zengler, K.; Knight, R. Establishing Microbial Composition Measurement Standards with Reference Frames. *Nat Commun* **2019**, 10. <https://doi.org/10.1038/s41467-019-10656-5>.
- (63) Rodriguez-R, L. M.; Konstantinidis, K. T. Estimating Coverage in Metagenomic Data Sets and Why It Matters. *The ISME Journal* **2014**, 8 (11), 2349–2351. <https://doi.org/10.1038/ismej.2014.76>.

- (64) Sczyrba, A.; Hofmann, P.; Belmann, P.; Koslicki, D.; Janssen, S.; Dröge, J.; Gregor, I.; Majda, S.; Fiedler, J.; Dahms, E.; Bremges, A.; Fritz, A.; Garrido-Oter, R.; Jørgensen, T. S.; Shapiro, N.; Blood, P. D.; Gurevich, A.; Bai, Y.; Turaev, D.; DeMaere, M. Z.; Chikhi, R.; Nagarajan, N.; Quince, C.; Meyer, F.; Balvočiūtė, M.; Hansen, L. H.; Sørensen, S. J.; Chia, B. K. H.; Denis, B.; Froula, J. L.; Wang, Z.; Egan, R.; Don Kang, D.; Cook, J. J.; Deltel, C.; Beckstette, M.; Lemaitre, C.; Peterlongo, P.; Rizk, G.; Lavenier, D.; Wu, Y.-W.; Singer, S. W.; Jain, C.; Strous, M.; Klingenberg, H.; Meinicke, P.; Barton, M. D.; Lingner, T.; Lin, H.-H.; Liao, Y.-C.; Silva, G. G. Z.; Cuevas, D. A.; Edwards, R. A.; Saha, S.; Piro, V. C.; Renard, B. Y.; Pop, M.; Klenk, H.-P.; Göker, M.; Kyrpides, N. C.; Woyke, T.; Vorholt, J. A.; Schulze-Lefert, P.; Rubin, E. M.; Darling, A. E.; Rattei, T.; McHardy, A. C. Critical Assessment of Metagenome Interpretation—a Benchmark of Metagenomics Software. *Nature Methods* 2017, 14 (11), 1063–1071.  
<https://doi.org/10.1038/nmeth.4458>.
- (65) Ye, L.; Mei, R.; Liu, W.-T.; Ren, H.; Zhang, X.-X. Machine Learning-Aided Analyses of Thousands of Draft Genomes Reveal Specific Features of Activated Sludge Processes. *Microbiome* **2020**, 8 (1), 16. <https://doi.org/10.1186/s40168-020-0794-3>
- (66) Campanaro, S.; Treu, L.; Rodriguez-R, L. M.; Kovalovszki, A.; Ziels, R. M.; Maus, I.; Zhu, X.; Kougias, P. G.; Basile, A.; Luo, G.; Schlüter, A.; Konstantinidis, K. T.; Angelidaki, I. New Insights from the Biogas Microbiome by Comprehensive Genome-Resolved Metagenomics of Nearly 1600 Species Originating from Multiple Anaerobic Digesters. *Biotechnology for Biofuels* **2020**, 13 (1), 25. <https://doi.org/10.1186/s13068-020-01679-y>.
- (67) Almeida, A.; Nayfach, S.; Boland, M.; Strozzi, F.; Beracochea, M.; Shi, Z. J.; Pollard, K. S.; Sakharova, E.; Parks, D. H.; Hugenholtz, P.; Segata, N.; Kyrpides, N. C.; Finn, R. D. A Unified

- Catalog of 204,938 Reference Genomes from the Human Gut Microbiome. *Nat Biotechnol* **2021**, 39 (1), 105–114. <https://doi.org/10.1038/s41587-020-0603-3>.
- (68) Nayfach, S.; Roux, S.; Seshadri, R.; Udwyary, D.; Varghese, N.; Schulz, F.; Wu, D.; Paez-Espino, D.; Chen, I.-M.; Huntemann, M.; Palaniappan, K.; Ladau, J.; Mukherjee, S.; Reddy, T. B. K.; Nielsen, T.; Kirton, E.; Faria, J. P.; Edirisinghe, J. N.; Henry, C. S.; Jungbluth, S. P.; Chivian, D.; Dehal, P.; Wood-Charlson, E. M.; Arkin, A. P.; Tringe, S. G.; Visel, A.; Woyke, T.; Mouncey, N. J.; Ivanova, N. N.; Kyrpides, N. C.; Eloe-Fadrosh, E. A. A Genomic Catalog of Earth's Microbiomes. *Nature Biotechnology* **2021**, 39 (4), 499–509. <https://doi.org/10.1038/s41587-020-0718-6>.
- (69) Stewart, R. D.; Auffret, M. D.; Warr, A.; Walker, A. W.; Roehe, R.; Watson, M. Compendium of 4,941 Rumen Metagenome-Assembled Genomes for Rumen Microbiome Biology and Enzyme Discovery. *Nature Biotechnology* 2019, 37 (8), 953–961. <https://doi.org/10.1038/s41587-019-0202-3>.
- (70) Gilroy, R.; Ravi, A.; Getino, M.; Pursley, I.; Horton, D. L.; Alikhan, N.-F.; Baker, D.; Gharbi, K.; Hall, N.; Watson, M.; Adriaenssens, E. M.; Foster-Nyarko, E.; Jarju, S.; Secka, A.; Antonio, M.; Oren, A.; Chaudhuri, R. R.; La Razione, R.; Hildebrand, F.; Pallen, M. J. Extensive Microbial Diversity within the Chicken Gut Microbiome Revealed by Metagenomics and Culture. *PeerJ* 2021, 9, e10941. <https://doi.org/10.7717/peerj.10941>.
- (71) Chen, C.; Zhou, Y.; Fu, H.; Xiong, X.; Fang, S.; Jiang, H.; Wu, J.; Yang, H.; Gao, J.; Huang, L. Expanded Catalog of Microbial Genes and Metagenome-Assembled Genomes from the Pig Gut Microbiome. *Nat Commun* 2021, 12. <https://doi.org/10.1038/s41467-021-21295-0>.
- (72) VandeWalle, J. L.; Goetz, G. W.; Huse, S. M.; Morrison, H. G.; Sogin, M. L.; Hoffmann, R. G.; Yan, K.; McLellan, S. L. *Acinetobacter*, *Aeromonas* and *Trichococcus* Populations Dominate the



Microbial Community within Urban Sewer Infrastructure: Dominant Microbial Populations of Sewer Infrastructure. *Environmental Microbiology* **2012**, *14* (9), 2538–2552.

<https://doi.org/10.1111/j.1462-2920.2012.02757.x>.

(73) Collection System Investigation Microbial Source Tracking (CSI-MST): Applying Molecular Markers to Identify Sewer Infrastructure Failures. *Journal of Microbiological Methods* 2020, *178*, 106068. <https://doi.org/10.1016/j.mimet.2020.106068>.

(74) Li, L.; Nesme, J.; Quintela-Baluja, M.; Balboa, S.; Hashsham, S.; Williams, M. R.; Yu, Z.; Sørensen, S. J.; Graham, D. W.; Romalde, J. L.; Dechesne, A.; Smets, B. F. Extended-Spectrum  $\beta$ -Lactamase and Carbapenemase Genes Are Substantially and Sequentially Reduced during Conveyance and Treatment of Urban Sewage. *Environ. Sci. Technol.* 2021, *55* (9), 5939–5949. <https://doi.org/10.1021/acs.est.0c08548>.

(75) Hultman, J.; Tamminen, M.; Pärnänen, K.; Cairns, J.; Karkman, A.; Virta, M. Host Range of Antibiotic Resistance Genes in Wastewater Treatment Plant Influent and Effluent. *FEMS Microbiology Ecology* **2018**, *94* (fiy038). <https://doi.org/10.1093/femsec/fiy038>.

(76) Wendl, M. C.; Kota, K.; Weinstock, G. M.; Mitreva, M. Coverage Theories for Metagenomic DNA Sequencing Based on a Generalization of Stevens' Theorem. *J Math Biol* 2013, *67* (5), 1141–1161. <https://doi.org/10.1007/s00285-012-0586-x>.

(77) Ebinger, A.; Fischer, S.; Höper, D. A Theoretical and Generalized Approach for the Assessment of the Sample-Specific Limit of Detection for Clinical Metagenomics. *Computational and Structural Biotechnology Journal* 2021, *19*, 732–742. <https://doi.org/10.1016/j.csbj.2020.12.040>.

(78) Hull, N. M.; Ling, F.; Pinto, A. J.; Albertsen, M.; Jang, H. G.; Hong, P.-Y.; Konstantinidis, K. T.; LeChevallier, M.; Colwell, R. R.; Liu, W.-T. Drinking Water Microbiome Project: Is It Time? *Trends Microbiol* **2019**, *27* (8), 670–677. <https://doi.org/10.1016/j.tim.2019.03.011>.



**Table 1.** Summary of representative MAGs recovered in this study representing sewage-associated populations.

Population	Taxonomic Summary				Quality Summary					
	Confident Taxonomy (p<0.05)	Best match in MiGA TypeMat Database	Similarity (%)	Metric	Completeness (%)	Redundancy (%)	Length (Mbp)	N50 (bp)	CDs	GC (%)
01	Genus: <i>Arcobacter</i>	<i>Arcobacter cryaerophilus</i> GCA 002992955	92.8	ANI	87.7	1.9	1.38	7,214	1,519	28.77
03	Genus: <i>Acinetobacter</i>	<i>Acinetobacter johnsonii</i> NZ CP065666	96.5	ANI	78.3	0	1.99	6,506	2,157	41.90
04	Genus: <i>Aeromonas</i>	<i>Aeromonas caviae</i> GCA 000819785	93.5	ANI	56.6	0.9	2.99	6,625	3,099	61.78
13	Class: <i>Bacteroidia</i>	<i>Paludibacter propionici</i> genes WB4 NC 014734	55.1	AAI	51.9	1.9	0.80	4,680	764	39.63
15	Species: <i>A. caviae</i>	<i>Aeromonas caviae</i> GCA 000820265	98.0	ANI	40.6	0	1.57	4,876	1,684	61.79
18	Genus: <i>Cloacibacterium</i>	<i>Cloacibacterium rupense</i> GCA 014645495	88.2	ANI	61.3	3.8	1.58	5,371	1,596	33.27
19	Family: <i>Campylobacteraceae</i>	<i>Arcobacter suis</i> CECT 7833 NZ CP032100	72.1	AAI	49.1	0	0.95	5,098	1,130	28.60
28	Order: <i>Neisseriales</i>	<i>Rivicola pingtungensis</i> GCA 003201855	67.3	AAI	75.5	0	1.13	5,350	1,176	56.67
29	Genus: <i>Moraxella</i>	<i>Moraxella osloensis</i> GCA 001679175	95.4	ANI	75.5	0	1.83	9,146	1,726	44.48
30	Species: <i>A. temperans</i>	<i>Acidovorax temperans</i> GCA 006716905	97.3	ANI	91.5	0.9	2.80	8,597	2,816	63.59
33	Genus: <i>Flavobacterium</i>	<i>Flavobacterium succinicans</i> LMG 10402 GCA 000611675	87.3	ANI	88.7	2.8	2.81	10,562	2,699	35.43
43	Species: <i>P. copri</i>	<i>Prevotella copri</i> DSM 18205 GCA 009495405	97.1	ANI	52.8	0	2.36	11,303	1,981	46.62
44	Species: <i>B. vulgatus</i>	<i>Bacteroides vulgatus</i> ATCC 8482 NC 009614	99.0	ANI	49.1	0	2.67	5,144	2,496	41.90
47	Family: <i>Aeromonadaceae</i>	<i>Tolomonas auensis</i> DSM 9187 NC 012691	83.5	ANI	98.1	1.9	2.67	16,590	2,612	47.97
49	Species: <i>R. pingtungensis</i>	<i>Rivicola pingtungensis</i> GCA 003201855	97.5	ANI	46.2	0.9	2.03	8,236	2,031	62.89

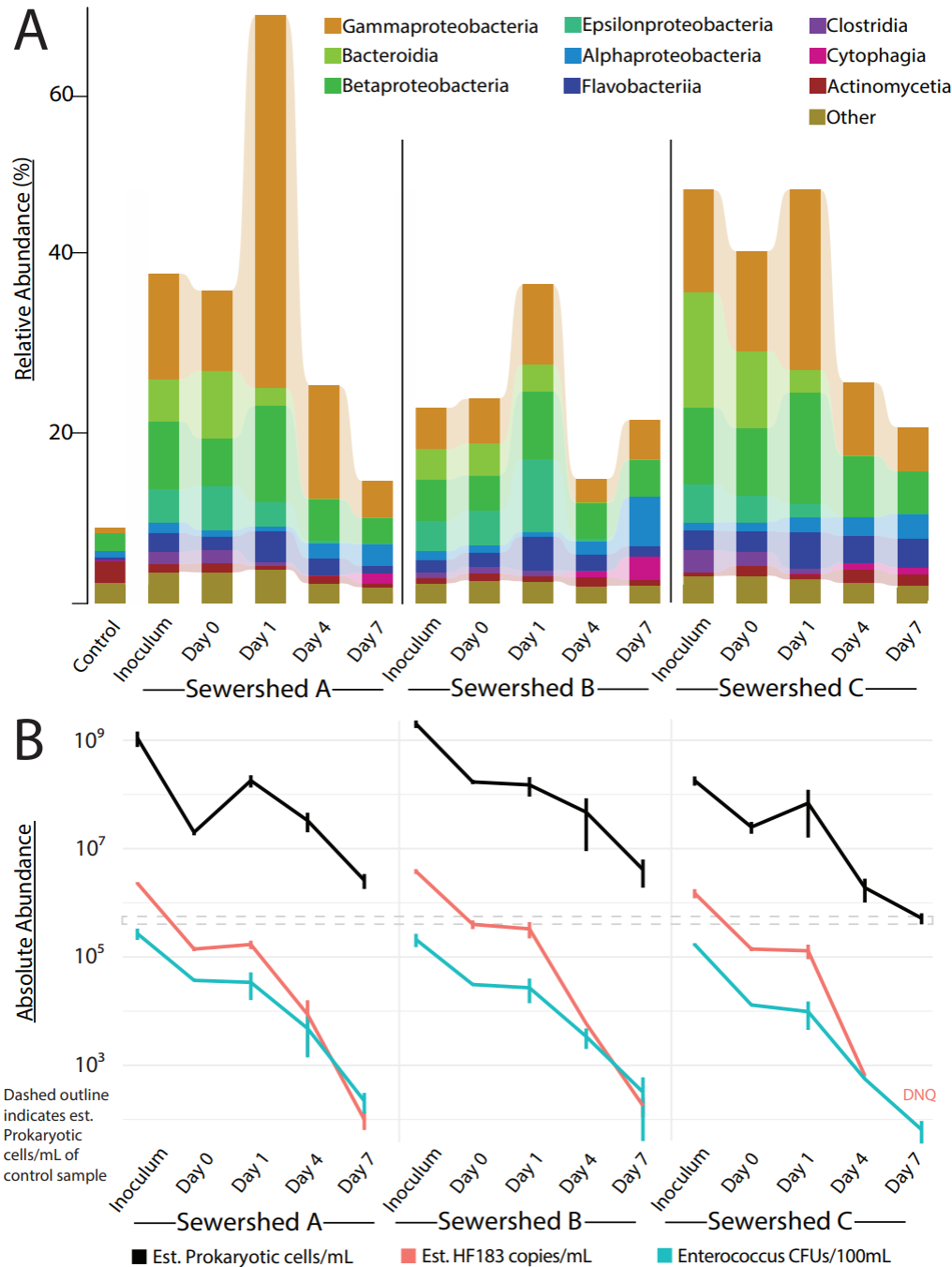


**Figure 1. Panel A:** Class level abundances across control, inoculum and timeseries for sewersheds A, B and C based on kmer classification by Kraken2 against a custom-built database of reference genomes. Total height of bars represents the percentage of kmers confidently classified to the corresponding taxon (Figure key). The maximum and minimum percentages of kmers confidently classified were 69.0% from Sewershed A day 1 and 8.9% from the control, respectively. **Panel B:** Estimated cell density, estimated HF183 copy concentration and Enterococci colony forming units (CFU) for the same samples. The dashed lines indicate the estimated cell density range for the control sample. HF183 was detected but not quantifiable (DNQ) for Sewershed C on day 7.

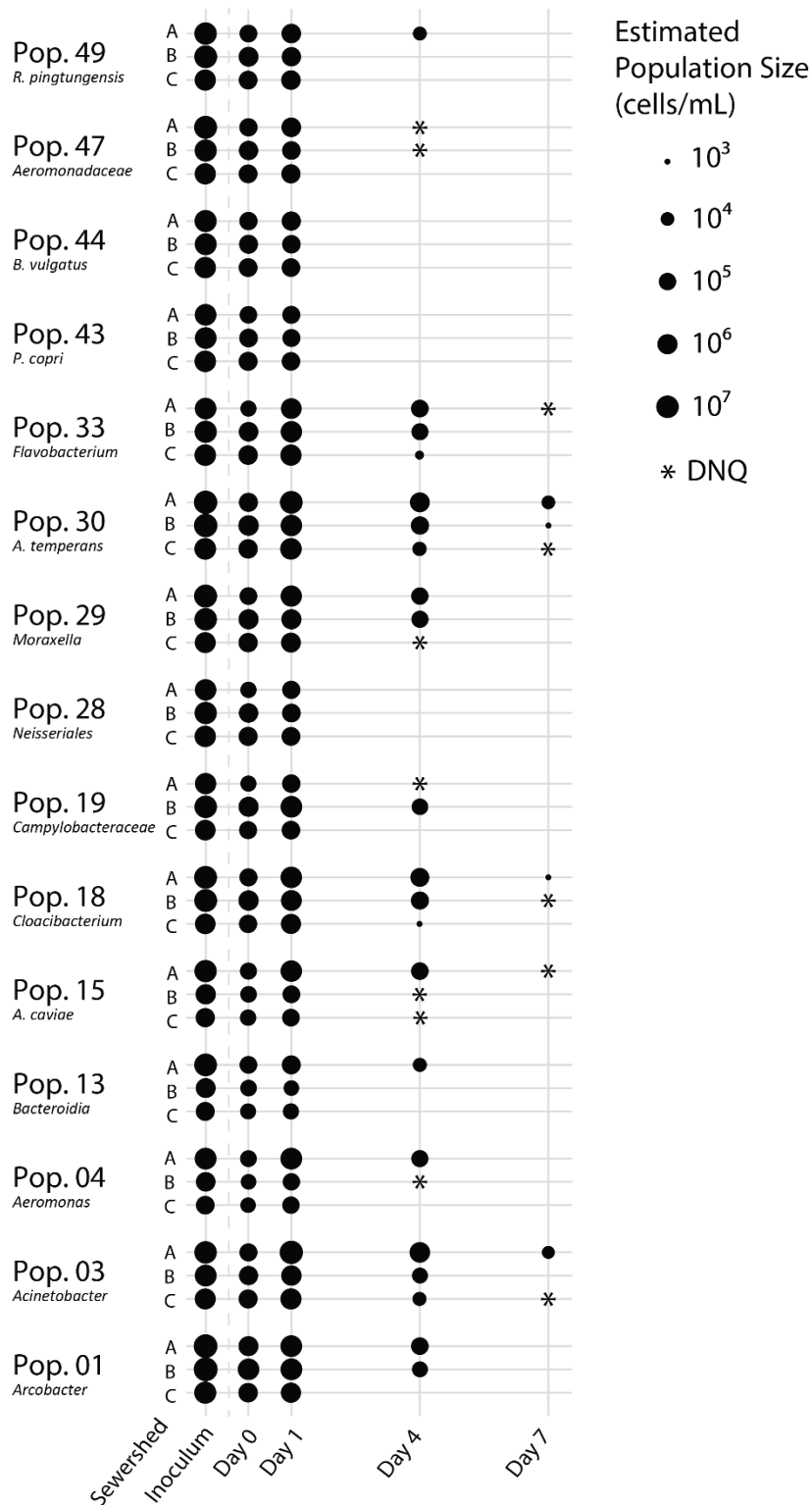


**Figure 2.** Estimated cell densities of sewage-associated populations across inoculum and timeseries samples. Cell densities (absolute abundances) were estimated as described in the Materials and Methods section.

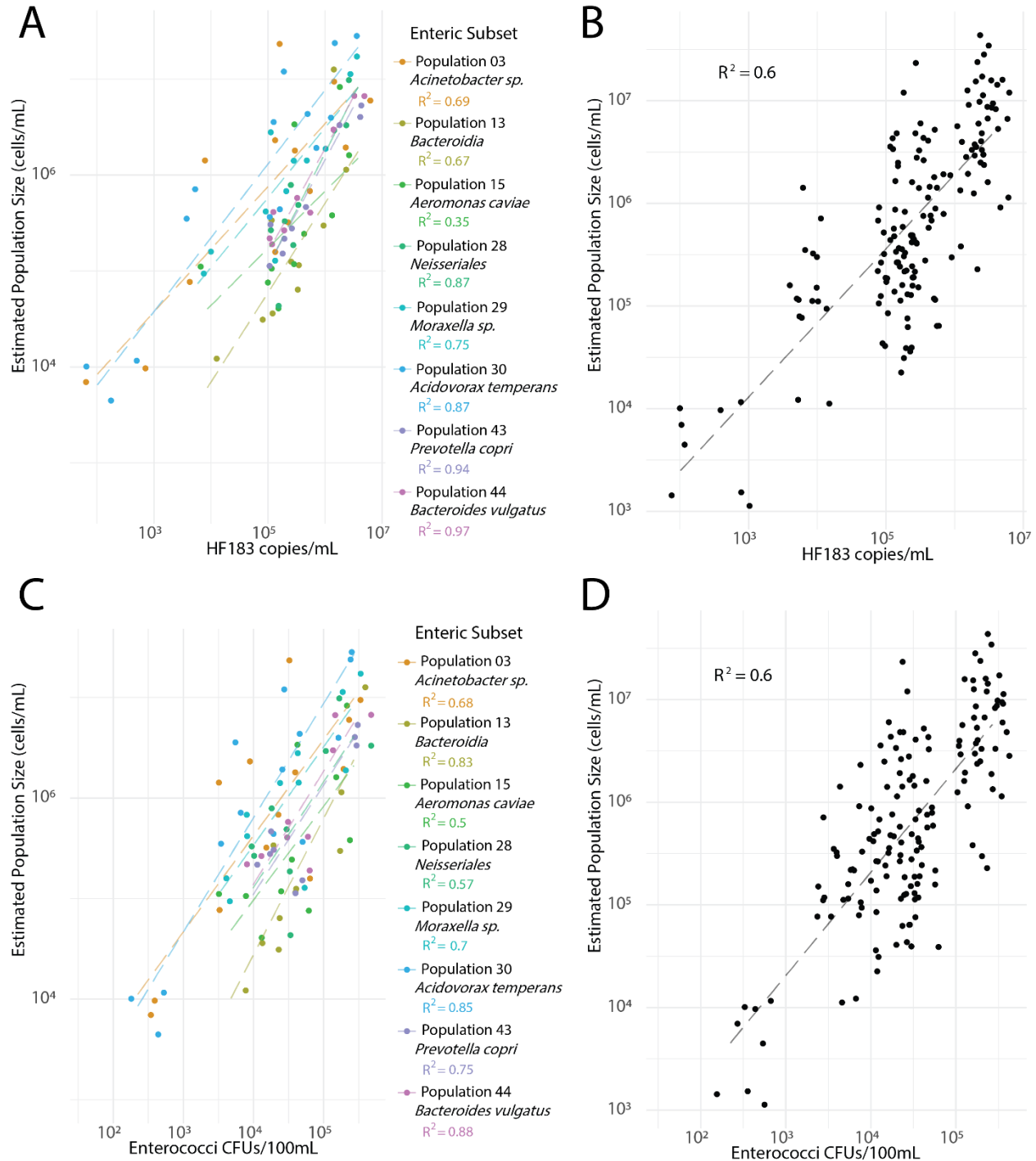


**Figure 3.** Log-log scatter plots of estimated population densities across inoculum and timeseries samples against HF183 and Enterococci concentrations. Lines of best fit are shown dashed with their associated coefficients. Panel A: HF183 copy number versus the concentration of sewage-associated populations likely to also be enteric (n=8). Panel B: HF183 copy number versus the concentration of all sewage-associated populations (n=15). Panel C: Enterococci concentration versus the concentration of sewage-associated populations likely to also be enteric (n=8). Panel D: Enterococci concentration versus the concentration of all sewage-associated populations (n=15).

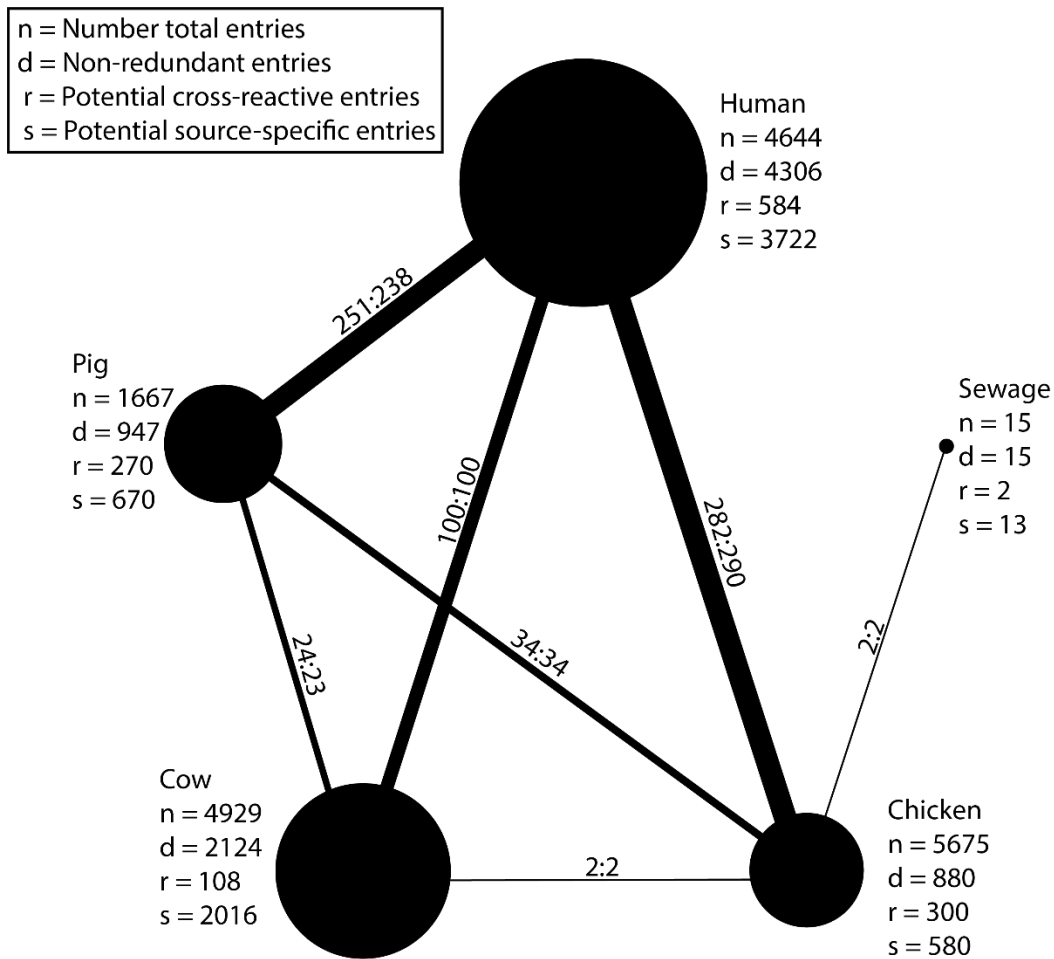


**Figure 4.** Overview of the curated genomic library for source attribution. Nodes represent sets of genomes recovered from public datasets of a given host microbiome, either “human”, “pig”, “cow”, and “chicken”. The “sewage” genomes shown here are those MAGs produced in this study. The radius of a node is proportional to the square root of the number of dereplicated genomes (d) remaining in the set following processing as described in the Methods section. Edges connecting nodes represent the amount of potentially cross-reactive genomes at the ANI  $\geq$  95% threshold level, and the line weights are drawn proportional to the square root of the largest number of these potentially cross-reactive matches (r). Ratios between nodes represent the number of matching genomes, with the value nearest a particular node representing the number of genomes from that dataset which matched across libraries.

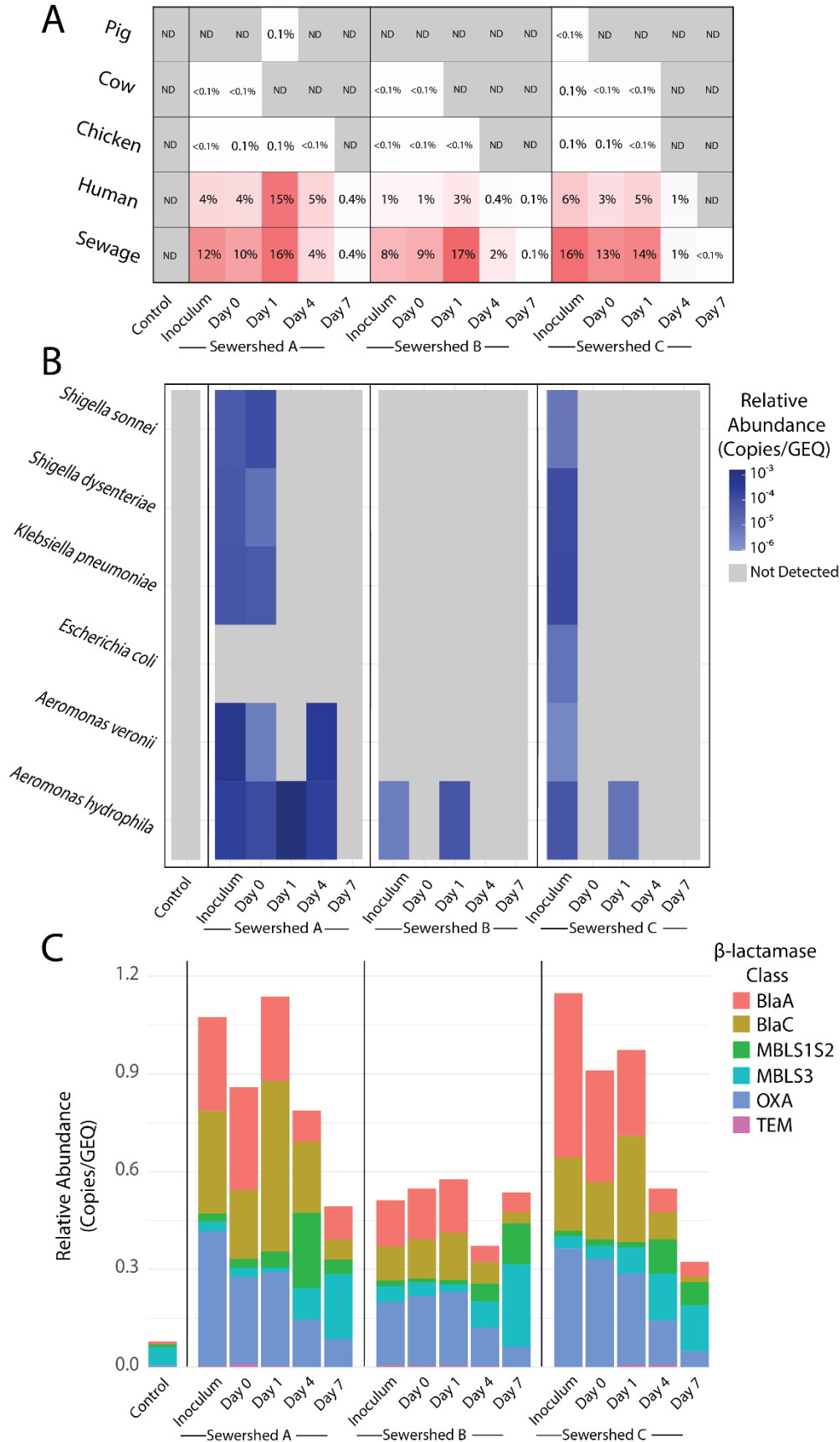




**Figure 5.** Abundance patterns of Source Tracking libraries, virulence factors and  $\beta$ -lactamase encoding genes across inoculum and timeseries metagenomes. All normalization was performed against genome equivalents (GEQ). **Panel A:** Source attribution and partitioning results based on reads mapped against MAGs curated for different fecal sources. Percentages represent estimates of the fraction of the prokaryotic population specifically belong to one of the fecal sources. **Panel B:** Virulence Factor (VF) gene abundance dynamics based on short reads mapping on experimentally verified VF reference nucleotide sequences (Figure key). **Panel C:**  $\beta$ -lactamase gene abundance dynamics across inoculum, timeseries and control metagenome based on Diamond --blastx searches of reads against reference ARG sequences and ROCKER model filtering of the resulting matches. Relative abundance is calculated by normalizing the average sequencing depth of each gene to GEQ after ROCKER filtering.